AD-A145 695   GUIDED-WAVE OPTIC DEVICES FOR INTEGRATED OPTIC   1/?
                INFORMATION PROCESSING(U) CALIFORNIA UNIV IRVINE DEPT
                OF ELECTRICAL ENGINEERING C S TSAI 08 AUG 84
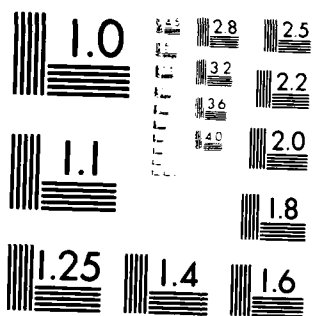UNCLASSIFIED   AFOSR-TR-84-0772 AFOSR-80-0288   F/G 20/6   NL

END
DATE
FILMED
10-84
DTIC

(4)

GUIDED-WAVE OPTIC DEVICES FOR INTEGRATED OPTIC INFORMATION PROCESSING

Annual Scientific Report

for

Air Force Office of Scientific Research

Grant No. AFOSR 80-0288

For the Period

30 January 1983 -- 30 January 1984

Prepared By

Chen S. Tsai, Principal Investigator
Professor of Electrical Engineering
University of California
Irvine, California   92717

84 09 17 007

GUIDED-WAVE OPTIC DEVICES FOR INTEGRATED OPTIC INFORMATION PROCESSING

Annual Scientific Report

Chen S. Tsai, Principal Investigator
Professor of Electrical Engineering
University of California
Irvine, California   92717

Table of Contents

Page No.

SECURITY CLASSIFICATION OF THIS PAGE *(When Data Entered)*

REPORT DOCUMENTATION PAGE	READ INSTRUCTIONS BEFORE COMPLETING FORM
1. REPORT NUMBER AFOSR-TR 2. GOVT ACCESSION NO. $A145695$	3. RECIPIENT'S CATALOG NUMBER
4. TITLE *(and Subtitle)* GUIDED-WAVE OPTIC DEVICES FOR INTEGRATED OPTIC INFORMATION PROCESSING	5. TYPE OF REPORT & PERIOD COVERED Annual Scientific Report 1/30/83 - 1/30/84
	6. PERFORMING ORG. REPORT NUMBER
7. AUTHOR(s) Professor Chen S. Tsai Principal Investigator	8. CONTRACT OR GRANT NUMBER(s) AFOSR Grant No. 80-0288
9. PERFORMING ORGANIZATION NAME AND ADDRESS Department of Electrical Engineering University of California Irvine, CA 92717	10. PROGRAM ELEMENT, PROJECT, TASK AREA & WORK UNIT NUMBERS $\sim 11c\lambda, 53c\gamma, B1$
11. CONTROLLING OFFICE NAME AND ADDRESS Air Force Office of Scientific Research (NE) Bolling AFB, D.C. 20332	12. REPORT DATE August 8, 1984
	13. NUMBER OF PAGES
14. MONITORING AGENCY NAME & ADDRESS *(if different from Controlling Office)* Air Force Office of Scientific Research (NE) Bolling AFB, D.C. 20332	15. SECURITY CLASS *(of this report)* Unclassified
	15a. DECLASSIFICATION DOWNGRADING SCHEDULE

16. DISTRIBUTION STATEMENT *(of this Report)*

Approved for public release; distribution unlimited

17. DISTRIBUTION STATEMENT *(of the abstract entered in Block 20, if different from Report)*

REPRODUCTION in whole or in part is permitted for any purpose of the United States Government

18. SUPPLEMENTARY NOTES

19. KEY WORDS *(Continue on reverse side if necessary and identify by block number)* Integrated and Guided-Wave Optics, Multichannel Communication and Signal Processing, AO Bragg Diffraction in ZnO/GaAs Waveguide, Magnetooptic Bragg Diffraction from Magnetostatic Surface Waves, Hybrid Integrated Optic Module, Radar Signal Processing

20. ABSTRACT *(Continue on reverse side if necessary and identify by block number)*

    Research efforts for this program year have been focused on the two topics as listed in the Introduction. Since both topical areas had been practically unexplored previously, a considerable amount of effort was spent on necessary preparations for in-depth studies of these two topics. The preparations include preliminary theoretical formulation of the problems, establishment of laboratory facilities for fabrication of the devices, and construction/assemblage of a large variety of required optical and RF equipment for

DD FORM 1 JAN 73 1473

20. ABSTRACT (Continued)

experimental verification of the basic concepts. Some very significant progress has been achieved in both topics. In the first topic, the theoretical analysis has uncovered a very efficient wideband Bragg diffraction configuration which involves a single-mode optical waveguide in the (001) plane of a GaAs substrate with the SAW propagating in the <100>- and <110>- directions. In the experimental phase, construction of an in-house sputtering system for fabrication of ZnO thin-film SAW transducers has been completed. This sputtering system was used to fabricate preliminary devices that have demonstrated high diffraction efficiency at 200 MHz SAW frequency. A paper which reports this progress was published recently.[1] A second paper was published in the Proceedings of the 1983 International Integrated Optic and Optical Fiber Communications Conference.[2]

In the second topic, through an all-out effort we have recently made significant progress in the experimental phase of research. We have most recently succeeded in the experimental observation of Non-Collinear Aniso-tropic Magnetooptic Diffraction from Magnetostatic Surface Waves in YIG/GGG Substrate. To the best of our knowledge, this is the first observation of its kind. We are in the process of improving the electronic instrumentation to facilitate detailed quantitative measurement. A paper was published in the Technical Digest of the 1984 Topical Meeting on Integrated and Guided-Wave Optics.[3]

GUIDED-WAVE OPTIC DEVICES FOR INTEGRATED OPTIC INFORMATION PROCESSING

Annual Scientific Report

Chen S. Tsai, Principal Investigator
Professor of Electrical Engineering
University of California
Irvine, California   92717

I.   INTRODUCTION

Integrated or Guided-Wave Optics is an emerging technology that has the
ultimate potential of integrating miniature optical components such as laser
light sources, modulators, switches, deflectors, lenses, prisms, and detectors
in a common substrate. The resultant integrated optic circuits and subsystems
are expected to have a number of advantages over the conventional bulk optical
systems in certain areas of applications. Some of the advantages include
smaller size and lighter weight, wider bandwidth, lesser electrical drive
power requirement, greater signal accessibility, and integratability. The
integrated optic circuits are also expected to possess advantages in stability,
reliability, ruggedness, and ultimate cost. It has been recognized for some
time that the most immediate applications of integrated optics lie in the
areas of wideband multichannel communications and signal processing (for both
civilian applications such as fiber optic systems and military hardwares such
as sensors and radars).

The general objectives of this research program are to study the basic
physical mechanisms/phenomenon of new and novel guided-wave devices with
application to wideband multichannel optical information processing. The
major tasks that have been carried out during this program year include
theoretical and experimental research on the following two major topics:

1. Wideband Guided-Wave Acoustooptic Interactions and Devices in GaAs-
    ZnO composite waveguides, and

2. Planar Guided-Wave Magneto-Optic Bragg Diffraction and Devices in
    YIG-GGG Waveguides.

Some very significant progress has been made in each research topic.

II. PROGRESS DURING CURRENT PROGRAM YEAR

A. Summary of Research Achievements

Research efforts for the current program year have been focused on the two topics as listed in the Introduction. Since both topical areas had been practically unexplored previously, a considerable amount of effort was spent on necessary preparations for in-depth studies of these two topics. The preparations include preliminary theoretical formulation of the problems, establishment of laboratory facilities for fabrication of the devices, and construction/assemblage of a large variety of required optical and RF equipment for experimental verification of the basic concepts. Some very significant progress has been achieved in both topics. In the first topic, the theoretical analysis has uncovered a very efficient wideband Bragg diffraction configuration which involves a single-mode optical waveguide in the (001) plane of a GaAs substrate with the SAW propagating in the <100>- and <110>- directions. In the experimental phase, construction of an in-house sputtering system for fabrication of ZnO thin-film SAW transducers has been completed. This sputtering system was used to fabricate preliminary devices that have demonstrated high diffraction efficiency at 200 MHz SAW frequency. A paper which reports this progress was published recently.[1] A second paper was published in the Proceedings of the 1983 International Integrated Optic and Optical Fiber Communications Conference.[2]

In the second topic, through an all-out effort we have recently made significant progress in the experimental phase of research. We have most recently succeeded in the experimental observation of Non-Collinear Anisotropic Magnetooptic Diffraction from Magnetostatic Surface Waves in YIG/GGG Substrate. To the best of our knowledge, this is the first observation of its kind. We are in the process of improving the electronic instrumentation to facilitate detailed quantitative measurement. A paper was published in the Technical Digest of the 1984 Topical Meeting on Integrated and Guided-Wave Optics.[3]

B. Research Progress

A detailed description of the progress and the achievements now follows:

1. Guided-Wave Acoustooptic Interactions and Devices in GaAs-ZnO Composite Waveguides

As indicated previously, integrated optic modules or circuits are expected to have a number of advantages over the conventional bulk counter-parts in certain areas of optical information processing applications.[4] At present, LiNbO$_3$ and GaAs are being identified as the two most promising substrate materials for eventual realization of integrated optic circuits. Clearly, in comparison to the LiNbO$_3$ substrate, the GaAs substrate provides a greater future potential for integration of active and passive components that are required in information processing and communications applications. One of the key components in such future GaAs integrated optic circuits is an efficient wideband acoustooptic (AO) modulator/deflector. This AFOSR-supported research project is aimed at developing this key component through a detailed theoretical and experimental study.

In the theoretical study, we have discovered an interaction configuration of great interest, namely the one with the SAW propagating along the <100> or <110> direction of the (001) plane of a GaAs substrate.[1] The analysis has shown that for SAW propagation directions such as those referred to above, numerical computations can be simplified considerably to generate a variety of design data unavailable heretofore. For example, it was shown in the last program year that very efficient wideband Bragg diffraction (1.6 GHz) could be achieved at 0.83 μm optical wavelength. We have recently obtained further theoretical results.[2] For example, as shown in Fig. 1(a) and 1(b), the topographical distribution of the induced changes in dielectric constant created by the <121>-propagating SAW in the (111)-substrate differs drastically from that created by the <100>-propagating SAW in the (001)-substrate. The nodal planes are seen to be flat in Fig. 1(a) but not in Fig. 1(b). The effects of this observation are reflected in the corresponding frequency dependence of the acoustic power-beam width product (PI) as shown in Fig. 2(a) and 2(b), exhibiting a phase cancellation in the former but not in the latter. However, from Fig. 3(a) and 3(b), the inherent AO Bragg bandwidth in the two interaction configurations are rather similar, again indicating the wideband capability with acoustooptic interactions in GaAs optical waveguides.

In the experimental study, we were convinced at the outset that establish-ment of an in-house RF sputtering facility for fabrication of a ZnO thin-film SAW transducer on the GaAs waveguide would greatly expedite this research. Consequently, a great deal of effort was made toward the construction of a

THE <121>—DIRECTION OF PROPAGATION
IN WAVELENGTH FOR (1̄1̄1̄)—SUBSTRATE

THE <100>—DIRECTION OF PROPAGATION
IN WAVELENGTH FOR {001}—SUBSTRATE

(b)
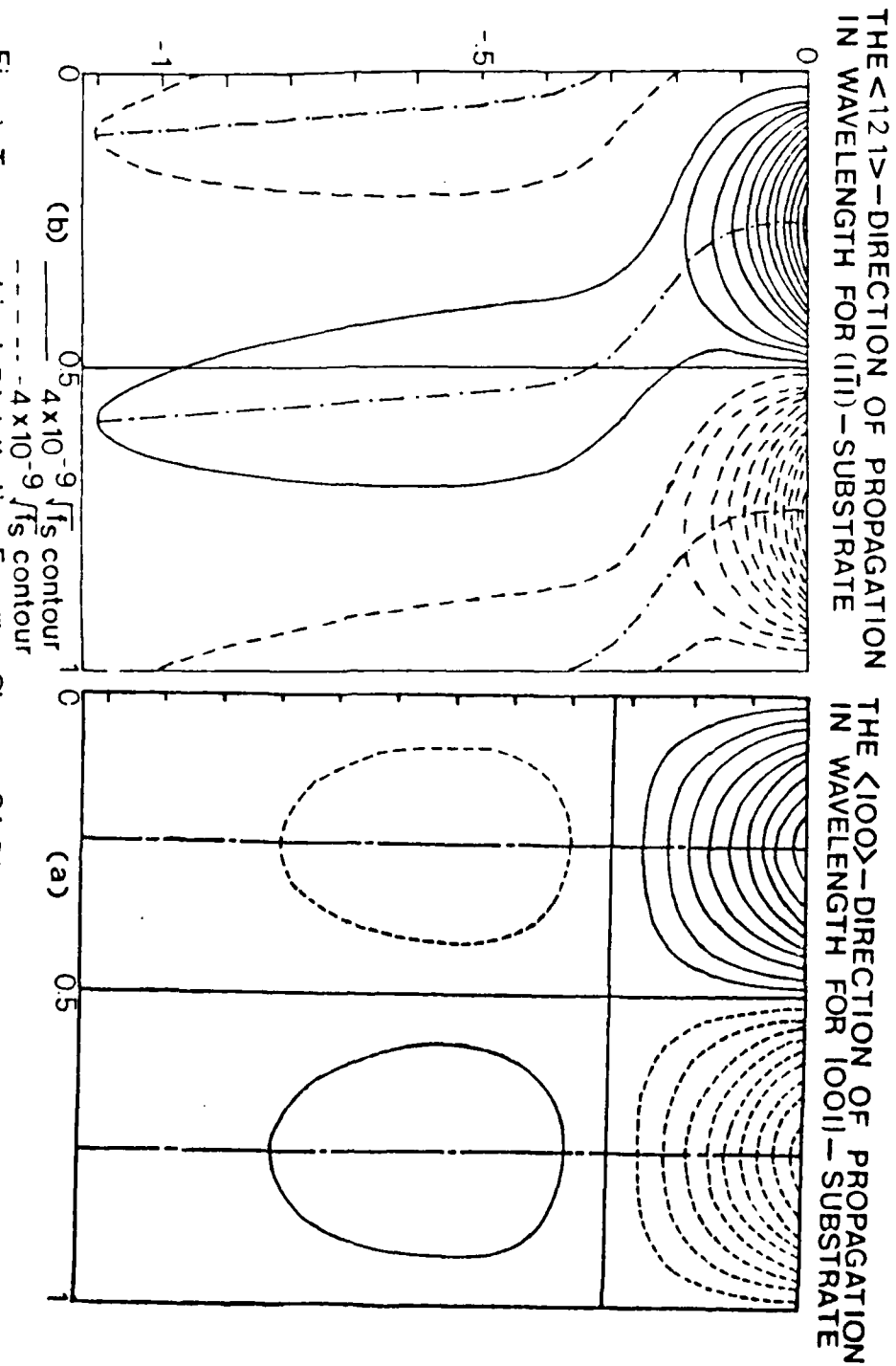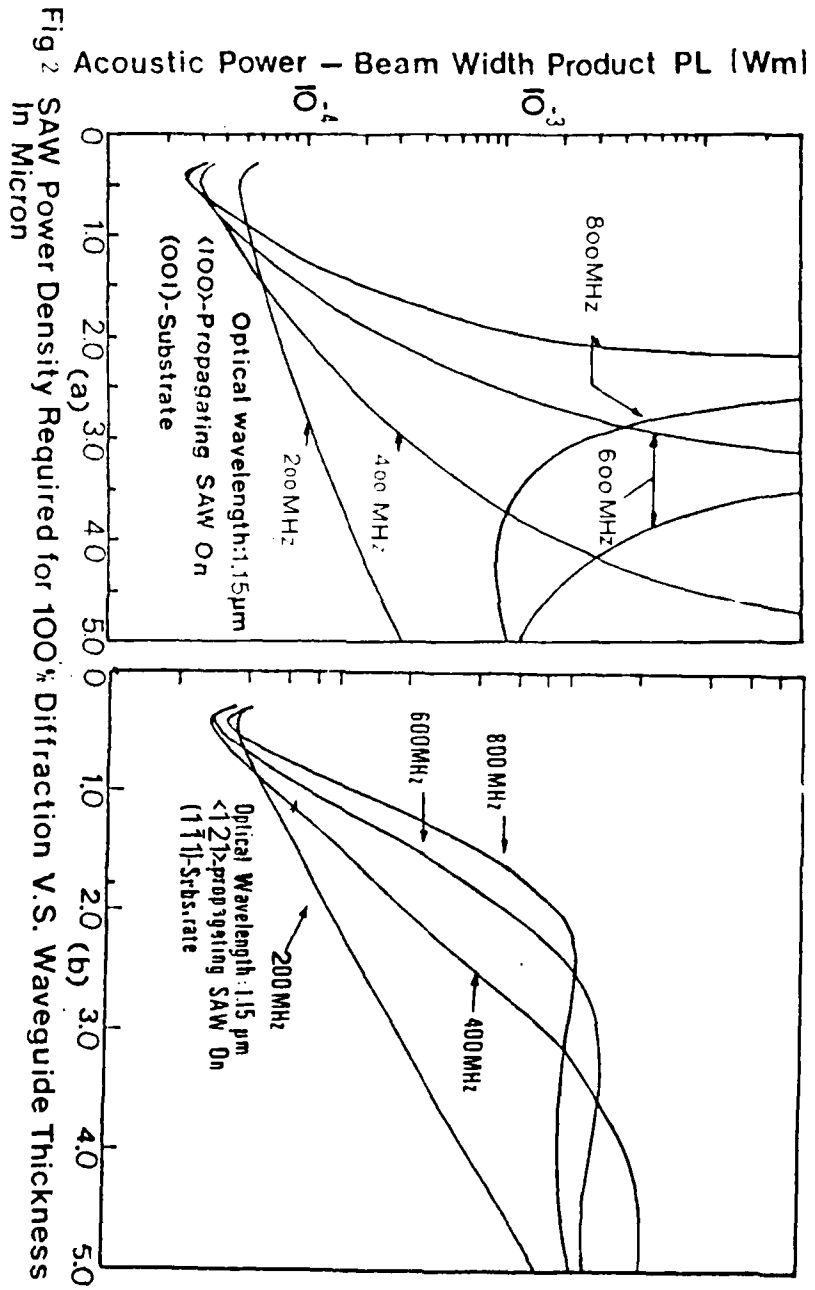
——— 4×10⁻⁹ √f̄s contour
– – – – –4×10⁻⁹ √f̄s contour

(a)

Fig. 1 Topographical Distribution For The Change Of Dielectric Constant In GaAs
Waveguide.The Vertical Axis In Both Figures Designates Waveguide Depth

Fig 2 SAW Power Density Required for 100% Diffraction V.S. Waveguide Thickness In Micron

Acoustic Power—Beam Width Product PL [Wm]

Optical Wavelength: 1.15 μm
〈100〉-Propagating SAW On
(001)-Substrate

10^{-4}

10^{-5}

o.6μm

o.3μm

o.7μm

$t_0 = 0.4$μm

o.5 μm

(a)

Optical Wavelength: 1.15 μm
〈121〉-Propagating SAW On
($1\bar{1}1$)-Substrate

10^{-4}

10^{-5}

0.4μm

0.5μm

0.3μm

0.6μm

0.7μm

(b)

ACOUSTIC FREQUENCY (MHz)
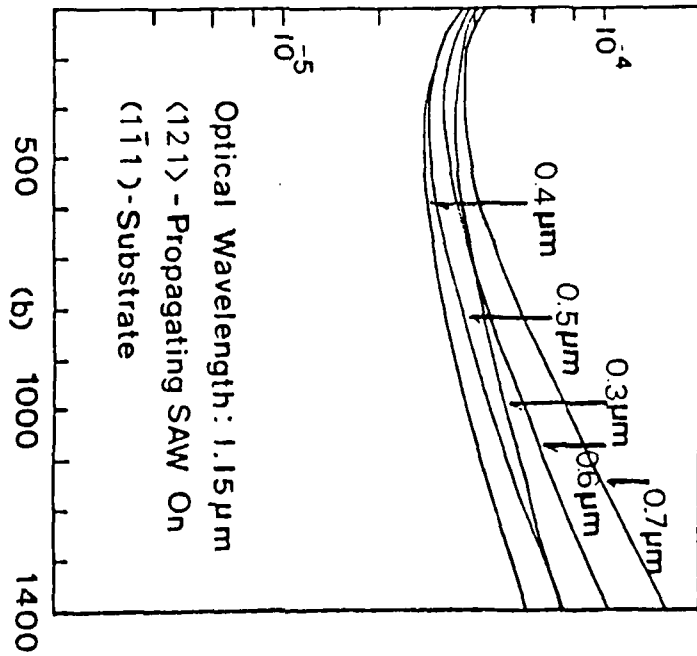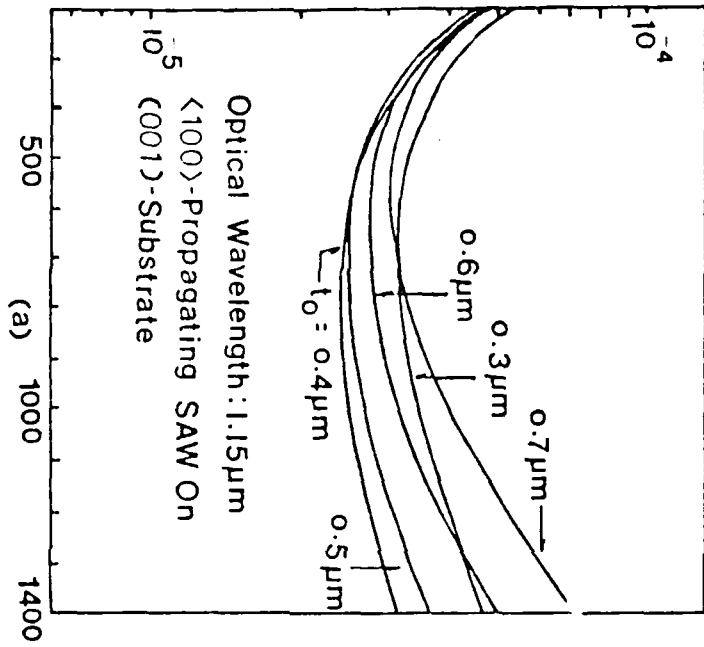
500   1000   1400

Fig 3 SAW Power Density Required V.S. Acoustic Frequency For TE_0–TE_0 100% Bragg
Diffraction In A Single—Mode Waveguide

FIGURE 4(a) RF SPUTTERING MACHINE

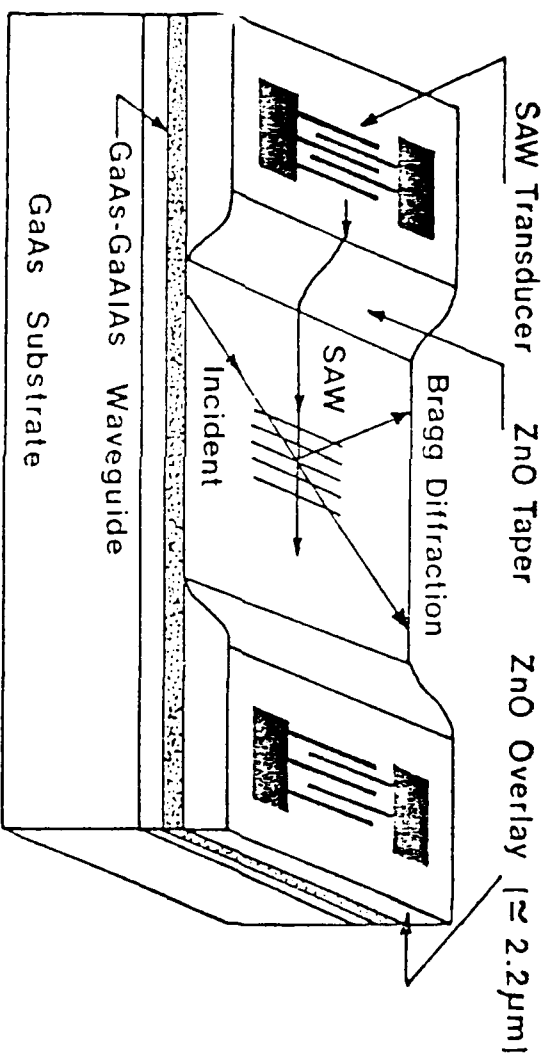FIGURE 4(b) DIFFUSION AND
MECHANICAL PUMPS

Fig. 5   Guided-Wave Acoustooptic Bragg Diffraction In
GaAs/GaAlAs-ZnO Composite Structure

modern sputtering system at the author's laboratory. This construction
has been completed (See Fig. 4). In fact, the system has gone through
several test runs and has already produced good-quality ZnO SAW trans-
ducers on glass substrates. Although at a lower degree of success, some
ZnO films were also deposited on GaAs waveguide substrates for transduction
of SAW at 200 MHz.

As a second step to the experimental study, the device configurations
as shown in Fig. 5 was recently fabricated. A 2-micron thick piezoelectric
ZnO film was first deposited on the GaAs waveguide by the sputtering system
referred to above. A 200 MHz transducer (20 finger pairs and 1 mm aperture)
was subsequently formed on the ZnO film. The very high refractive index of
GaAs, namely, 3.4 at 1.15 micron laser wavelength has made excitation of
guided-wave through prism coupling extremely difficult. Consequently, the
(110) cleaved plan of GaAs was used to edge-couple the light beam. This
preliminary AO Bragg cell has demonstrated high diffraction efficiency,
namely, 50% diffraction at 47 mw RF drive power.[1] This preliminary result
is in fair agreement with the theoretical prediction. Improvements in the
qualities of the optical waveguide and SAW transducer should produce even
better results and closer agreement with the theoretical predictions.

2. Guided-Wave Magneto-Optic Bragg Diffraction and Devices in YIG/GGG
   Waveguides

This project concerns theoretical and experimental studies on "Inter-
actions between Guided-Optical Waves and Magnetostatic Surface Waves in
Thin-Film YIG/GGG Composite With Applications to Optical Information Process-
ing." An interaction configuration of particular interest that has been
identified is shown in Fig. 6. Note that in this non-collinear configuration,
the propagation direction of the lightwave is nearly orthogonal to that of the
magnetostatic surface wave (MSSW), in contrast to the co-llinear configuration
that was reported recently.[5] Like guided-wave acoustooptics, non-collinear
guided-wave magnetooptic interactions are expected to be much more versatile
in application that the collinear interactions. The MSSW excited in the YIG
film by means of a short-circuited metallic strip serves to induce changes
in the refractive index. We suggested in the original proposal that the
grating created by this induced index changes then diffracts the incident
light in a manner similar to the diffraction due to the well-known acousto-
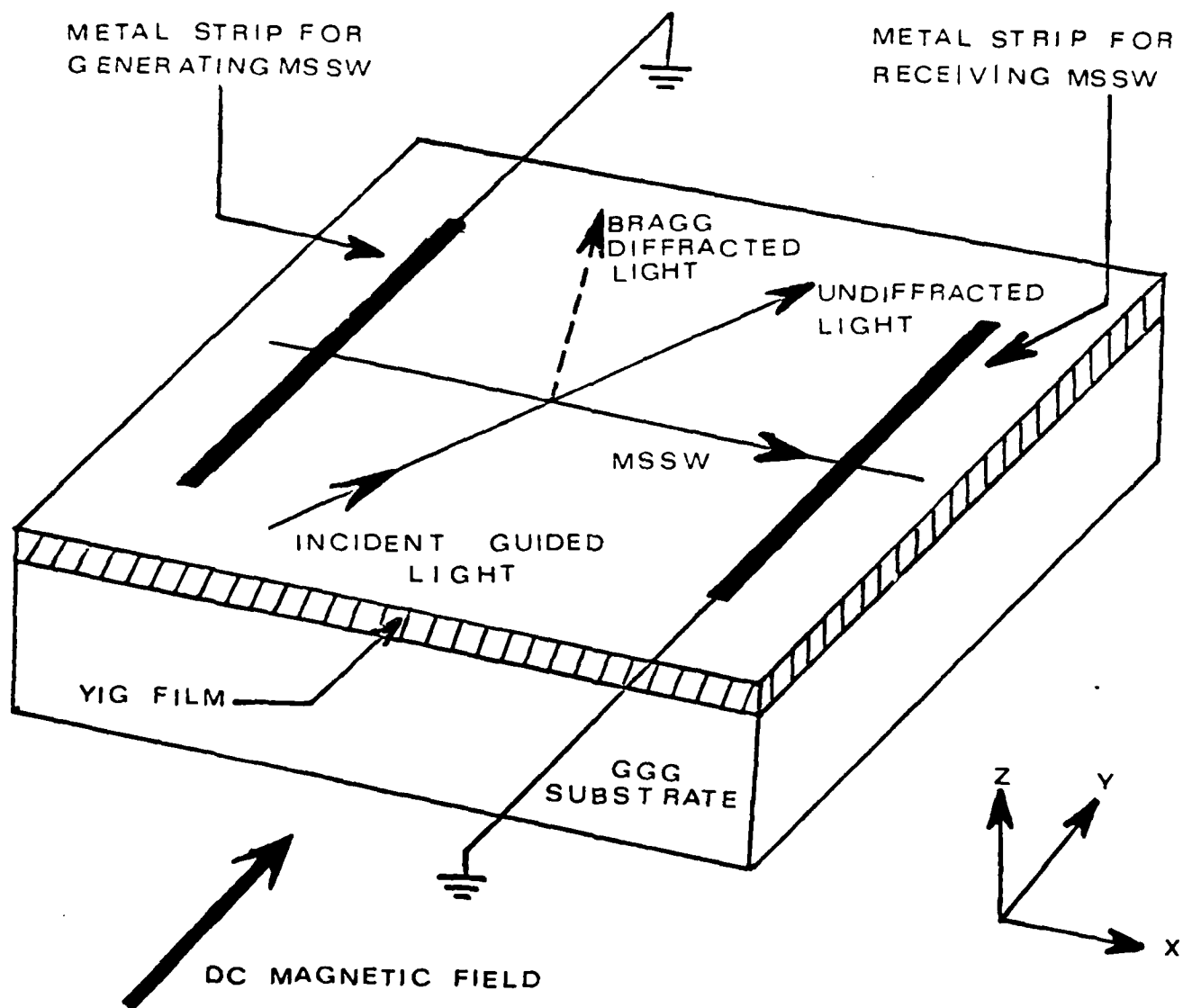optic effect. However, the resultant magnetooptic devices will have the

FIG 6 GEOMETRY FOR PLANAR GUIDED-WAVE MAGNETO-OPTIC
BRAGG DIFFRACTION FROM MAGNETOSTATIC SURFACE WAVE

following unique characteristics in comparison to the existing acoustooptic devices:

1. very high and electrically tunable RF center frequency (2 to 20 GHz) enables the devices to operate at the actual operation frequency of radar and communication systems.

2. design and fabrication of efficient and wideband transducers for the MSSW are considerably simpler,

3. the propagation loss of the MSSW is much lower than that of the conventional SAW, especially at the upper range of the frequencies referred to in item 1, and

4. the combined nondispersive and dispersive properties of the MSSW provides a potential for a new class of signal processing devices.

Since this non-collinear guided-wave magnetooptic diffraction had been totally unexplored and the experimental setup for observation of this diffraction phenomena requires a large assortment of microwave and optical components, a considerable amount of time and effort has been spent in building and assembling of the experimental setup from scratch. The setup used for this experimental observation is shown in Fig. 7. The YIG/GGG substrate furnished by Drs. Howard Glass and Larry Adkins of Rockwell International was first brought in contact with an alumina plate which has a pair of parallel metallic strips deposited on it for excitation and detection of the MSSW (See Fig. 8). The composite sample was then mounted on a specially-made holder and inserted in the air gap of an electromagnet. A microwave signal centered at 4.0 GHz was then applied to one of the metal strips to excite the MSSW.[6-8] The MSSW generated propagates in the plane of the sample and is detected by the other metal strip. By changing the magnitude of the D-C magnetic field, the frequency of the MSSW has been tuned from 3.0 GHz to 5.0 GHz, demonstrating a bandwidth of 2.0 GHz.

Following the successful excitation of the MSSW, an attempt was undertaken to excite guided-optical waves using a He-Ne laser at 6328 Å as the optical insertion loss of the sample was found to be too excessive at this visible light wavelength to obtain any meaningful result. Subsequently, a Jodon He-Ne Laser at 1.15 μm wavelength was purchased using the funds provided by the University. This laser arrived finally after a long delay and was recently put into operation after repairment. In order to minimize
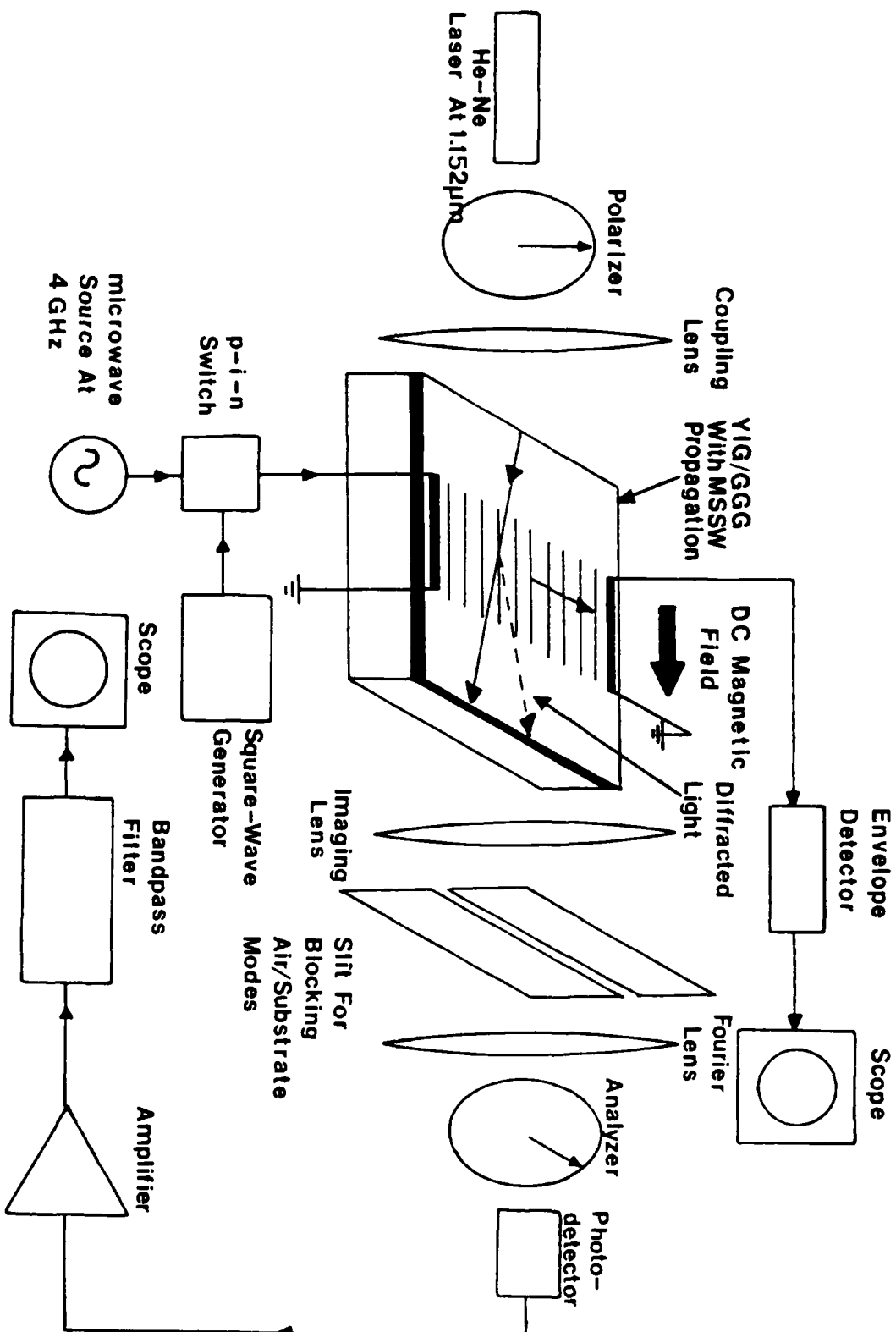
Fig. 7 **Schematic Diagram For Guided-Wave Noncollinear Anisotropic Magneto-optical Diffraction From Magnetostatic Surface Wave**
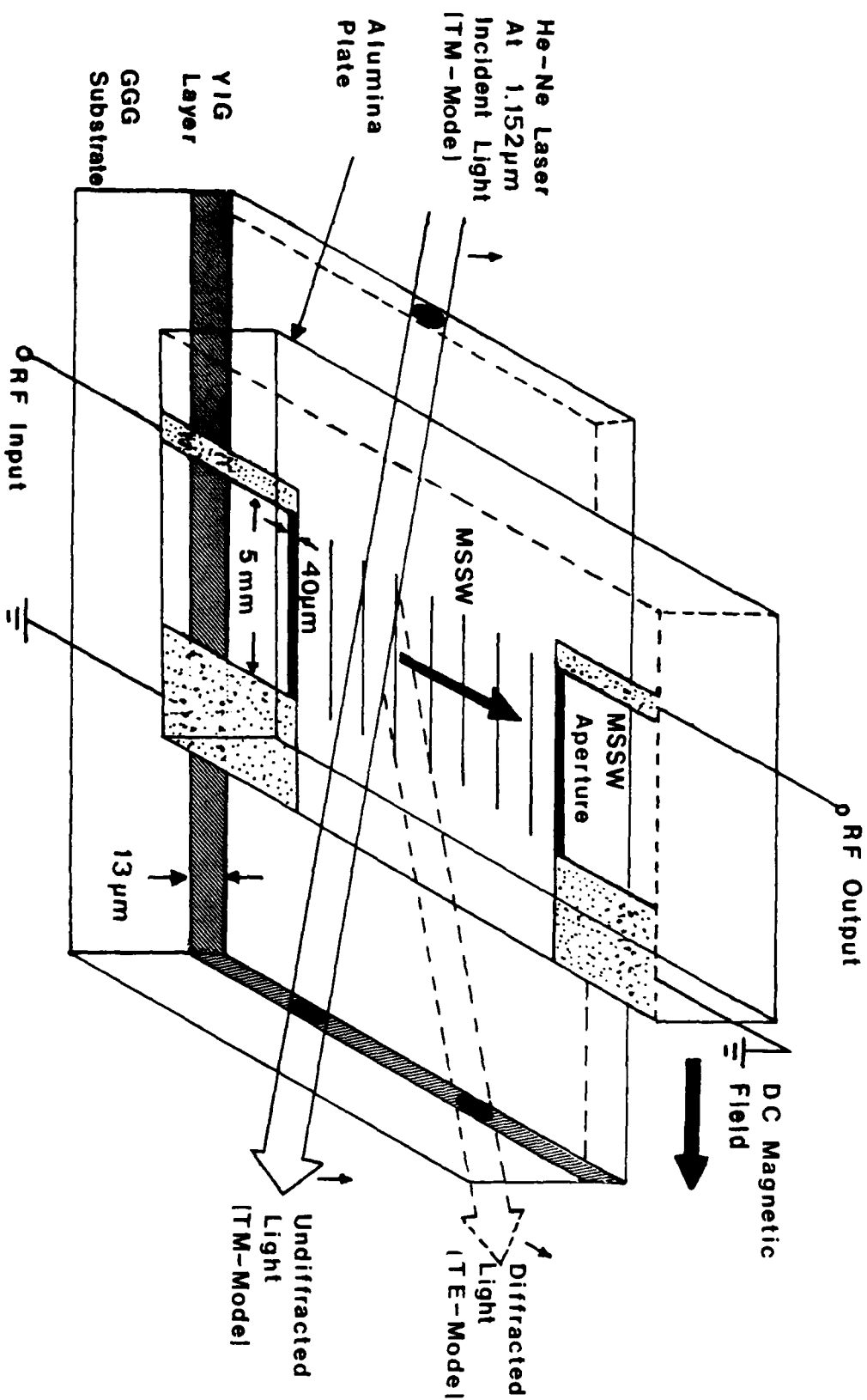
Fig. 8 **Device Geometry For Guided-Wave Noncollinear Anisotropic Magneto-Optical Diffraction Using Magnetostatic Surface Wave**
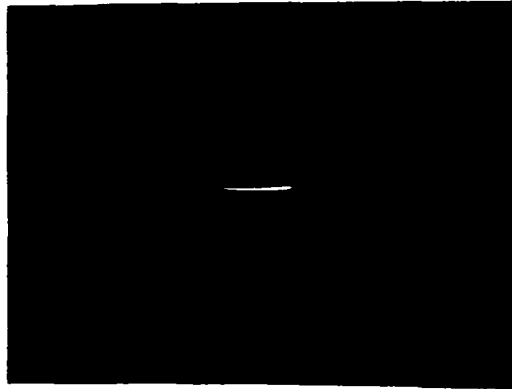
Fig. 9   Output Beam Profile Of A TM-Mode Guided Light In A
         YIG/GGG Waveguide Excited By Edge-Coupling Using A
         Cylindrical Lens
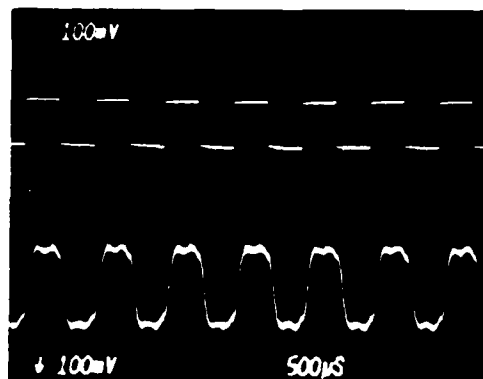
Fig. 10   Non-collinear Planar Guided-Wave Magneto-
          optic Diffraction From Magnetostatic Sur-
          face Wave: 1.4 KC Square-Wave Modulated
          Magnetostatic Surface Wave At 3.9 GHz
          Carrier Frequency (Top Trace); Diffracted
          Light Waveform (Bottom Trace).

the optical insertion loss, the dimension of the YIG/GGG substrate along the optical propagation path was chosen to be as small as 5.0 mm. This small dimension also necessitated usage of edge-coupling for excitation of guided optical modes in the YIG waveguide. Typical beam profiles of the guided-mode generated in a 13 μm YIG film as recorded in an IR image converter is shown in Fig. 9.

Following the successful generation of both the MSSW and the guided-optical wave, the incident angle of the guided light beam was adjusted to maximize the output of the IR detector. We have found that the polariza-ation of the diffracted light is orthogonal to that of the incident light. Fig. 10 shows the oscilloscope trace of the detector output together with that of the corresponding square-wave modulation and the MSSW at 3.9 GHz. Clearly, we have for the first time succeeded in observation of Guided-Wave Non-Collinear Magnetooptic Diffraction Using Magnetostatic Surface Waves. We are in the process of improving the electronic instrumentation to facilitate optimization of the detected signal for detailed quantitative measurement.

III. REFERENCES

1. O. Yamazaki, C. S. Tsai, M. Umeda, et al, "Guided-Wave Acoustooptic Interaction in GaAs-ZnO Composite Structure," Proceedings of 1982 Ultrasonics Symposium, pp. 418-421, IEEE Cat. No. 82CH1823-4.

2. C. J. Lii, C. C. Lee, O. Yamazaki, L. S. Yap, K. Wasa, J. Merz, and C. S. Tsai, "Efficient Wideband Acoustooptic Bragg Diffraction in GaAs-GaAlAs Waveguide Structure," Proceedings of the 1983 International Conference on Integrated Optics and Optical Fiber Communications, June 27-30, Tokuo, Japan, pp. 252-253.

3. C. S. Tsai, D. Young, L. Adkins, C. C. Lee, and H. Glass, "Planar Guided-Wave Magnetooptic Diffraction from Magnetostatic Surface Waves in YIG/GGG Waveguides," 1984 Topical Meeting on Integrated and Guided-Wave Optics, Technical Digest, pp. TuB3-1 to -4, IEEE Cat. No. 84-CH1997-6.

4. C. S. Tsai, "Guided-Wave Acoustooptic Bragg Modulators for Wideband Integrated Optic Communications and Signal Processings," Invited Paper, IEEE Trans. on Circuits and Systems, Special Issue on Integrated and Guide Wave Optical Circuits and Systems, Vol. CAS-26, 1072-1098 (Dec. 1979).

5. A. D. Fisher, J. N. Lee, E. S. Gaynor, and A. B. Tveten, "Diffraction of Guided Optical Waves in Magnetostatic Wave Delay Lines," 1982 Ultrasonics Symposium Proceedings, IEEE Cat. No. 82CH1823-4, pp. 541-546.

6. J. D. Adam and J. H. Collins, "Microwave Magnetostatic Delay Devices Based on Epitaxial Yttrium Iron Garnet, "Proc. IEEE, 64, 794-800 (May 1976).

7. J. M. Owens, R. L. Carter, C. V. Smith and J. H. Collins, Magnetostatic Waves, Microwave SAW," 1980 IEEE Ultrasonics Symp. Proc., Cat. No. 80CH1602-2, 506-513.

8. L. R. Adkins and H. L. Glass, "Propagation of Magnetostatic Surfact Waves in Multiple Magnetic Layer Structures," Electronics Letters, Vol. 16.

9. K. Y. Liao, C. C. Lee, and C. S. Tsai, "Time-Integrating Correlator Using Guided-Wave Anisotropic Acoustooptic Bragg Diffraction and

Hybrid Integration," Sixth Topical Meeting on Integrated and Guided-Wave Optics, Jan. 6-8, 1982. Technical Digest, pp. WA4-1 to -4, IEEE Cat. No. 82CH1719-4.

10. R. E. Camley, T. S. Rahman, and D. L. Mills, "Theory of Light Scattering by the Spin-Wave Excitations of Thin Ferromagnetic Film," Physical Review B, Vol. 23, No. 3, 1-19, (Feb. 1, 1982).

11. S. Ushioda, "Light Scattering Spectroscopy of Surface Electromagnetic Waves in Solids," Progress in Optics, Vol. 19, pp. 139-210, 1982. Edited by E. Wolf.

IV. <u>RESEARCH IMPACTS AND MOST RECENT PUBLICATIONS RESULTING FROM AFOSR SUPPORT</u>

A. <u>Research Impacts</u>

1. The paper entitled, "Efficient Wideband Acoustooptic Bragg Diffraction in GaAs-GaAlAs Waveguide Structure," was very well received at the <u>1983 International Conference on Integrated Optics and Optical Fiber Communications</u>. Quite a few researchers expressed interest in this work.

2. The paper entitled, "Planar Guided-Wave Magnetooptic Diffraction from Magnetostatic Surface Waves in YIG-GGG Waveguides," generated a great deal of interest among the attendees at the <u>1984 Topical Meeting on Integrated and Guided-Wave Optics</u>. Successful demonstration of efficient wideband diffraction and electronic tuning of the RF carrier frequency of the resultant magnetooptic device was much appreciated. It is well recognized that the resultant magnetooptic Bragg cells should possess potential advantages over the acoustooptic Bragg cells in wideband real-time signal processing applications.

B. <u>Most Recent and Future Publications</u>

1. K. Y. Liao, C. C. Lee, and C. S. Tsai, "Time-Integrating Correlation Using Guided-Wave Anisotropic Acoustooptic Bragg Diffraction and Hybrid Integration," <u>Sixth Topical Meeting on Integrated and Guided-Wave Optics</u>, Jan. 6-8, 1982. Technical Digest, pp. WA4-1 to -4, IEEE Cat. No. 83CH171904.

2. C. S. Tsai, C. C. Lee, and K. Y. Liao, "RF Correlation With Integrated Acoustooptic Modules," <u>1982 Wescon Convention Records</u>, Session 26, <u>Real-Time Signal Processing Using Integrated Optics Technology</u>, pp. 26-3-1 to 26-3-4.

3. C. C. Lee, K. Y. Liao, and C. S. Tsai, "Acoustooptic Time-Integrating Correlator Using Hybrid Integrated Optics," <u>1982 IEEE Ultrasonics Symp. Proc.</u>, pp. 405-407, IEEE Cat. No. 82CH1823-4.

4. O. Yamazaki, C. S. Tsai, M. Umeda, et al, "Guided-Wave Acoustooptic Interaction in GaAs-ZnO Composite Structure," <u>Proceedings of 1982 Ultrasonics Symposium</u>, pp. 418-421, IEEE Cat. No. 82CH18323-4.

5. C. J. Lii, C. C. Lee, O. Yamazaki, L. S. Yap, K. Wasa, J. Merz, and C. S. Tsai, "Efficient Wideband Acoustooptic Bragg Diffraction

in GaAs-GaAlAs Waveguide Structure," Proceedings of 1983
International Conference on Integrated Optics and Optical Fiber
Communications, June 27-30, Tokyo, Japan, pp. 252-253.

6. C. S. Tsai, "Hybrid Integrated Optic Modules for Real-Time Signal
Processing," Invited Paper, presented at 10th International Optical
Computing Conference, April 6-8, 1983, MIT, MA.

7. C. S. Tsai, "Hybrid Integrated Optic Modules for Real-Time Signal
Processing," Proc. of NASA Optical Information Processing Conference,
NASA Conference Publication No. 2302, pp. 149-164, Aug. 1983.

8. C. S. Tsai, D. Young, C. C. Lee, L. Adkins, and H. Glass, "Planar
Guided-Wave Magnetooptic Diffraction from Magnetostatic Surface
Waves in YIG/GGG Waveguides," 1984 Topical Meeting on Integrated and
Guided-Wave Optics, Technical Digest, pp. TuB3-1 to -4, IEEE Cat.
No. 84CH1997-6.

V. PROFESSIONAL PERSONNEL ASSOCIATED WITH THE RESEARCH EFFORT

1. Dr. Chen S. Tsai, Principal Investigator
   Professor of Electrical Engineering
   University of California, Irvine

2. Dr. Chin C. Lee, Research Specialist
   University of California, Irvine

3. Dr. Osamu Yamazaki, Visiting Scholar
   Matsushita Electric. Co., Japan

4. Dr. Jim Merz
   Professor of Electrical Engineering
   University of California, Santa Barbara

5. Dr. Larry Adkins
   Member of Technical Staff
   Rockwell International
   Anaheim, CA

6. Dr. Howard Glass
   Member of Technical Staff
   Rockwell International
   Anaheim, CA

7. K. Y. Liao, Research Assistant
   School of Engineering
   University of California, Irvine

8. M. Umeda, Research Assistant
   School of Engineering
   University of California, Irvine

9. L. S. Yap, Research Assistant
   School of Engineering
   University of California, Irvine

10. J. K. Wang, Research Assistant
    School of Engineering
    University of California, Irvine

11. C. J. Lii, Research Assistant
    School of Engineering
    University of California, Irvine

12. D. Young, Research Assistant
    School of Engineering
    University of California, Irvine

VI. ADVANCED DEGREES AWARDED

Ph.D. Thesis

K. Y. Liao, Thesis Title: Wide-Bank Real-Time Signal Processing
Using Integrated Optics (April 1983).

M.S. Thesis

Y. S. Yap, Thesis Title: Study of ZnO Films with Application to
Guided-Wave Acoustooptic Interactions in GaAs Substrate
(Feb. 1983).

C. J. Lii, Thesis Title: Efficient Wideband Acoustooptic Bragg
Diffraction in GaAs-GaAlAs Waveguide Structure (Oct. 1983).

D. Young, Thesis Title: Efficient Wideband Acoustooptic Bragg
by Magnetostatic Surface Waves in YIG-GGG Waveguides
(Oct. 1984).

SEVENTH TOPICAL MEETING ON

INTEGRATED AND GUIDED-WAVE OPTICS

A digest of technical papers presented at the Seventh Topical Meeting on
Integrated and Guided-Wave Optics, April 24-26, 1984, Orlando Hyatt Hotel, Kissimmee, Florida.

Sponsored by:

Quantum Electronics and Applications Society
of the Institute of Electrical and Electronics Engineers

Optical Society of America

PLANAR GUIDED-WAVE MAGNETOOPTIC DIFFRACTION BY MAGNETOSTATIC
SURFACE WAVES IN YIG/GGG WAVEGUIDES*

C.S. Tsai, D. Young, L. Adkins⁻, C.C. Lee, and H. Glass
Department of Electrical Engineering
University of California
Irvine, CA 92717

Summary

Modulation and switching of light waves in Yttrium iron garnet (YIG)-
Gadolinium gallium garnet (GGG) waveguides using Farady rotation[1], and light
propagation and mode-conversion in a thin-film dielectric waveguide using magneto-
optic YIG substrate[2,3] had been studied in detail. More recently, propagation
and mode-conversion in a YIG/GGG waveguide with an isotropic top layer using
Faraday rotation was also analyzed.[4] In this paper we report on wideband modu-
ulation at multigigahertz (2 to 7 GHz) center frequency that results from planar
magnetooptic diffraction by magnetostatic surface waves in the YIG/GGG waveguide.

Magnetostatic surface waves (MSSW) results from propagation of electron spin
precession around an external DC magnetic field and has its energy confined mostly
in a thin-film of ferromagnetic material such as YIG on a suitable substrate such
as GGG. The MSSW can be readily and efficiently generated by applying a micro-
wave signal to a short-circuited metallic strip which is brought in close prox-
imity to the ferromagnetic film. The center frequency of the MSSW can be simply
tuned, typically from 1.0 to as high as 20 GHz, by varying the frequency of the
microwave signal generator and the DC magnetic field.

Similar to the surface acoustic waves (SAW) that induce changes in the
refractive index through its stress or strain field, the MSSW can also induce
changes in the refractive index of the ferromagnetic film through its RF magnetic
field. Consequently, a moving optical grating is created in the waveguide through
propagation of the MSSW. The periodicity of the grating is determined by the
dispersion characteristic of the MSSW. The optical grating created can cause dif-
fraction of an incident guided-light wave in the plane of the waveguide if phase
matching condition is satisfied among the incident light wave, the diffracted
light wave, and the MSSW. Clearly, such planar guided-wave structure possesses
the potential for miniaturization and integration of the resultant devices in com-

parison to the one that utilizes unguided-light waves and magnetostatic bulk waves.[5-8] The general configuration of the guided-wave magnetooptic diffraction described above is depicted in Fig. 1. Note that the collinear configuration reported recently[9] in which all three wave vectors of the incident-, diffracted-, and the magnetostatic surface-waves lie in one direction ($\theta_i = 90°$) is a special case of the non-collinear configuration to be emphasized in this paper. As in planar guided-wave acoustooptic diffraction,[10] device application with non-collinear configuration is expected to be more versatile than the collinear configuration.

The detailed arrangement and basic dimensions of the YIG/GGG waveguide and the MSSW transducer used in our experimental study are shown in Fig. 2. The YIG film was fabricated using liquid phase epitaxy. A pair of parallel metallic strips with a separation of 5.0mm in between was deposited on an alumina substrate. The electrode pair was then brought to near contact with the YIG film by flipping the alumina substrate. One electrode was used to excite while the other was used to detect and measure the MSSW. Efficient excitation of the MSSW was accomplished over a frequency band as large as 2 to 7 GHz. The corresponding DC magnetic field was 200 to 1700 Gauss. Excitation, propagation, and detection of single-mode optical waves at 1.152 μm wavelength were facilitated using edge coupling. Planar guided-wave magnetooptic diffraction from the MSSW was observed with the non-collinear configuration as well as the collinear configuration. Fig. 3 shows a 1.4KC modulated MSSW at 7.0 GHz carrier frequency and the corresponding modulated light intensity. In this particular experiment the optical modulation was facilitated with non-collinear interaction of the TE_0- and the TM_0-mode optical waves and the MSSW. To the best of our knowledge such non-collinear planar guided-wave magnetooptic diffraction was observed for the first time.[11]

The measured diffracted light power was shown to depend linearly on the input RF drive power for a power range of at least 15 dB. At 4.0 GHz center frequency the diffraction efficiency was measured to be 2.5% at 1.0 watt RF drive power. A -3 dB magnetooptic bandwidth of 500 MHz centering at 4.0 GHz was also measured by varing the carrier frequency of the MSSW but with the DC magnetic field fixed at 803 Gauss.

In summary, wideband non-collinear planar guided-wave magnetooptic diffraction from 2 to 7 GHz magnetostatic surface waves has been observed and measured in detail for the first time. This magnetooptic diffraction phenomenon should result in a number of integrated optic devices for wideband communications and signal processing applications. Inteaction configurations, physical mechanisms, and

detailed experimental results will be presented.

Dr. C.T. Lee participated in the research described in this paper when the research was first initiated some three years ago.

References

1. P.K. Tien et al, Appl. Phys. Lett., 21, 394 (1972).

2. S. Wang et al, J. Appl. Phys., 43, 1862 (April 1972).

3. J. Warner, IEEE Trans. Microwave Theory Tech., MTT-21, 769 (Dec. 1973).

4. K. Taki et al, Trans. Inst. Electron. Commun. Eng. Japan; E63, 754 (Oct. 1980).

5. B.A. Auld and D.A. Wilson, J. Appl. Phys., 38, 3331 (July 1967).

6. B.A. Auld and D.A. Wilson, Appl. Phys. Lett., 11, 368 (Dec. 1967).

7. J.H. Collins and D.A. Wilson, Appl. Phys. Lett., 12, 331 (May 1968).

8. H.L. Hu and F.R. Morgenthaler, Appl. Phys. Lett., 18, 307 (April 1, 1971).

9. A.D. Fisher et al, Appl. Phys. Lett., 41, 770 (Nov. 1982).

10. C.S. Tsai, IEEE Trans. Circuits and Systems, Vol. CAS-26, 1072 (Dec. 1979).

11. First Observation of Non-Collinear Planar Guided-Wave Magnetooptic Diffraction was Disclosed at the NASA Optical Information Processing Conference II, Aug. 30-31, 1983, NASA Langley Research Center, Virginia in a presentation entitled, "Hybrid Integrated Optic Modules for Real-Time Signal Processing" by C.S. Tsai.
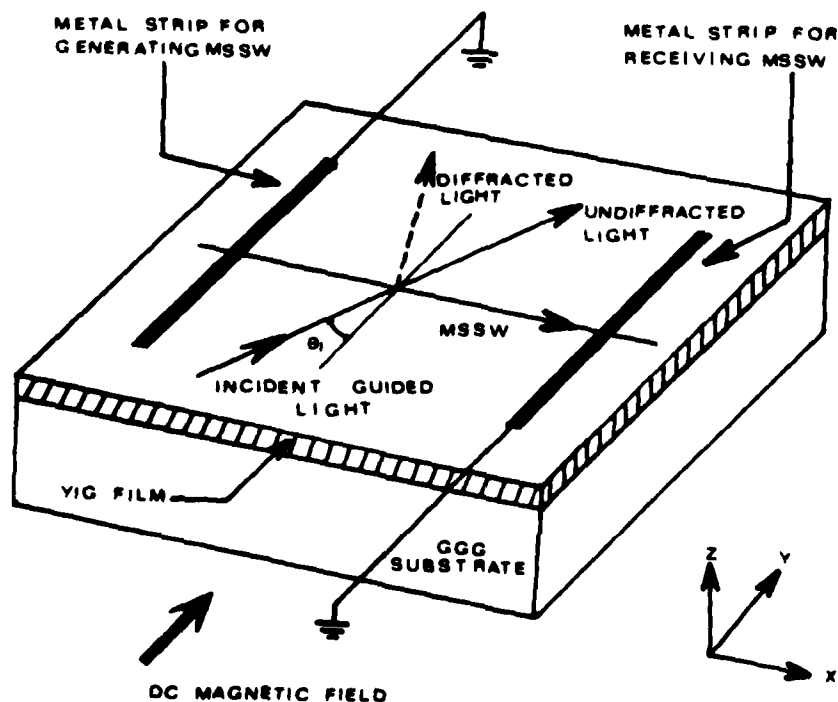
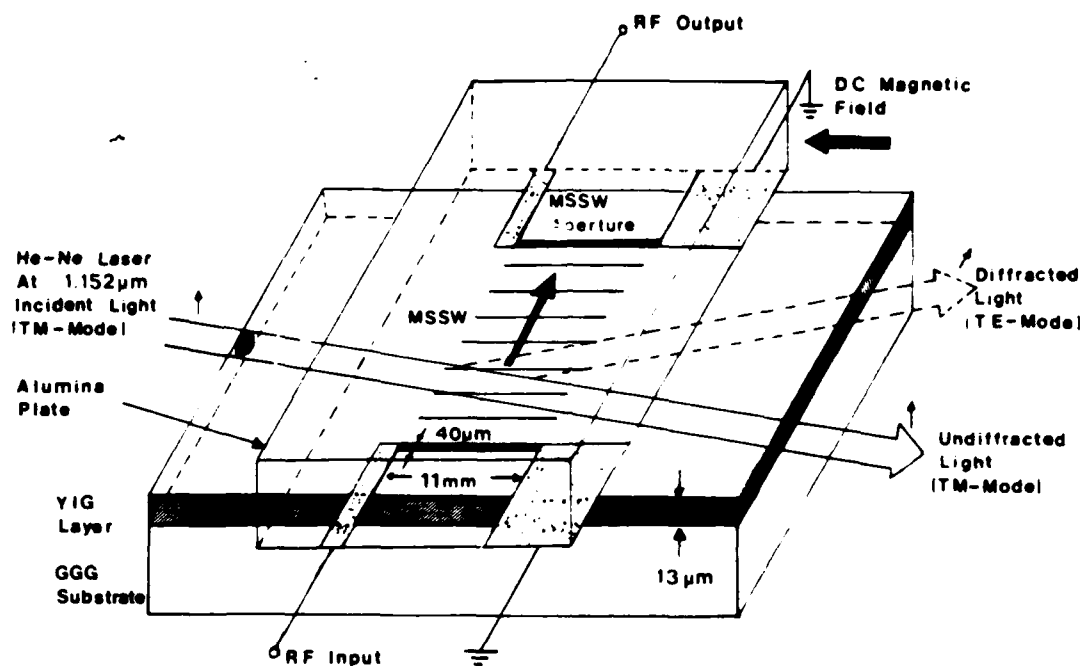FIG.1 NON-COLLINEAR PLANAR GUIDED-WAVE MAGNETO-OPTIC DIFFRACTION FROM MAGNETOSTATIC SURFACE WAVE

FIG.2 Device Geometry For Guided-Wave Noncollinear Anisotropic
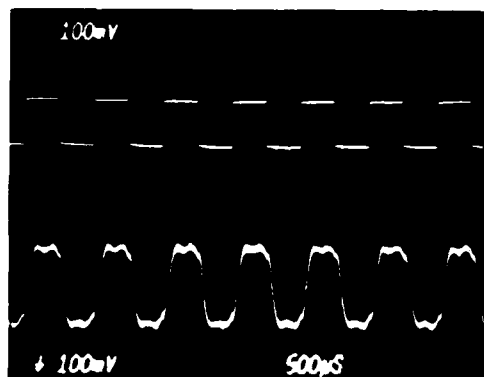Magneto-Optical Diffraction Using Magnetostatic Surface Wave

Fig. 3   Non-collinear Planar Guided-Wave Magneto-
optic Diffraction From Magnetostatic Sur-
face Wave: 1.4 KC Square-Wave Modulated
Magnetostatic Surface Wave At 7.0 GHz
Carrier Frequency (Top Trace); Diffracted
Light Waveform (Bottom Trace).

Optical Information Processing for Aerospace Applications II

Compiled by Robert L. Stermer
Langley Research Center

NASA

National Aeronautics
and Space Administration

Scientific and Technical
Information Branch

1984

HYBRID INTEGRATED OPTIC MODULES FOR REAL-TIME SIGNAL PROCESSING*

Chen S. Tsai
Department of Electrical Engineering
University of California, Irvine

ABSTRACT

This paper reports the most recent progress on four relatively new hybrid integrated optic device modules in $LiNbO_3$ waveguides and one in YIG/GGG waveguide that are currently being studied at the author's laboratory. The five hybrid modules include a time-integrating acoustooptic correlator, a channel waveguide acoustooptic frequency shifter/modulator, an electrooptic channel waveguide TIR modulator/switch, an electrooptic analog-to-digital converter using a Fabry-Perot modulator array, and a noncollinear magnetooptic modulator using magnetostatic surface waves. All of these devices possess the desirable characteristics of very large bandwidth (GHz or higher), very small substrate size along the optical path (typically 1.5 cm or less), single-mode optical propagation, and low drive power requirement. The devices utilize either acoustooptic, electrooptic or magnetooptic effects in planar or channel waveguides and, therefore, act as efficient interface devices between a light wave and temporal signals. Major areas of application lie in wideband multichannel optical real-time signal processing and communications. Some of the specific applications include spectral analysis and correlation of RF signals, fiber-optic sensing, optical computing and multiport switching/routing, and analog-to-digital conversion of wide RF signals. The common technical problems that require further research and development include fabrication yield, fiber-waveguide and diode laser-waveguide couplings, and resistance to optical damage.

INTRODUCTION

Recent advancements on the performances of individual guided-wave optical devices, basic building blocks, their interconnections, coupling to and from waveguide, and specific real-world applications have been quite significant. Together with the recent progress on fabrication of miniature laser sources, waveguide lenses and photodetectors, integration of all passive and active components on a single substrate or a small number of substrates is becoming a reality. This emerging technology can be utilized to implement integrated optic modules for wideband multichannel optical communications and signal processing systems. Clearly, such future integrated optic modules should share a number of attractive features, such as very large bandwidth, low electrical drive power, small size, light weight, less susceptibility to environmental effects, and potentially less cost in fabrication. In this paper five new hybrid integrated optic modules currently being explored at the author's laboratory are reported together with most recent results.

TIME-INTEGRATING ACOUSTOOPTIC CORRELATOR

Time-integrating correlation of RF signals using bulk-wave isotropic acousto-optic (AO) Bragg diffraction has become a subject of great interest because of its applications in radar signal processing and communications. Some encouraging results with the experiments which utilize guided-wave isotropic Bragg diffraction was reported earlier (ref. 1). Subsequently, hybrid and monolithic structures for integrated optic implementations were suggested (ref. 2). In a conventional configuration that utilizes either bulk-wave or guide-wave isotropic Bragg diffraction, a pair of imaging lenses and a spatial filter are used to separate the diffracted light beam from the undiffracted light beam. We are presently exploring a new and novel hybrid structure which utilizes guided-wave anisotropic Bragg diffraction and hybrid integration (See Fig. 1) (ref. 3). This new structure can conveniently incorporate a thin-film polarizer to separate the diffracted light from the undiffracted light prior to detection and, therefore, eliminate the need of imaging lenses and spatial filter. As a result, the acoustooptic time-integrating correlator is not only much smaller in dimension along the optical path and capable of providing a larger time window and a lower optical insertion loss, but it is also easier to implement in integrated optic format. A laser diode and a thin-film polarizer/photodetector array (CCPD) composite are butt-coupled to the input and the output end faces of a Y-cut LiNbO$_3$ plate (2mm x 12mm x 15.4mm), respectively. A single geodesic lens (with 8mm focal length) is used to collimate the input light beam prior to interaction with the surface acoustic wave (SAW). The SAW propagates at 5 degrees from the X-axis of the LiNbO$_3$ plate to facilitate anisotropic Bragg diffraction between TE$_0$ and TM$_0$ modes. In operation, the correlation between the two signals S$_1$(t) and S$_2$(t) is performed by separately modulating the laser diode and the RF carrier to the SAW transducer. Finally, the time-integrating correlation waveform is read out from the detector array by the charged-coupled device.

The preliminary experiment carried out earlier with the correlator of incomplete hybrid integration at 0.6328µm wavelength and the SAW at 391 MHz center frequency had demonstrated a bandwidth of 60 MHz, a time bandwidth product of 4.2 x 10^5, and a dynamic range of -27dB (ref. 3). A considerably larger bandwidth can be realized as it is now possible to design and fabricate GHz bandwidth planar acoustooptic Bragg cells (ref. 4) and it is also possible to modulate the diode laser at GHz rates. Fig. 2 shows the LiNbO$_3$ substrate of the module with the geodesic lens located at the center and the SAW transducer at the right end. Most recently, complete hybrid integration using a diode laser at 0.78µm wavelength and the SAW at 314 MHz center frequency was accomplished. Some preliminary results have been obtained but the aperture of the collimated guided-light beam needs to be enlarged in order to perform a meaningful evaluation of this hybrid integrated correlator module.

CHANNEL WAVEGUIDE ACOUSTOOPTIC DEFLECTOR/MODULATOR

While planar waveguide AO devices have already reached some degree of sophistication and found immediate applications (ref. 5), channel waveguide AO devices, which result from acoustooptic deflection in channel waveguides, have only started to receive interest and attention (ref. 6). This interest was motivated by the fact that comparable cross sections of the channel waveguide and the optical fiber would greatly facilitate the interfacing of the resultant AO channel devices with fiber optic systems. One interaction configuration of particular interest is shown in Fig. 3. Two identical channel waveguides in a Y-cut LiNbO$_3$ substrate are crossed at an angle

to form a $2\Delta n$ straight intersection (ref. 7). Unlike the conventional Δn intersection, the retractive index change in the crossover region is twice that in the other parts of the channel waveguide. As a result, the light wave is also guided in the crossover region and the crosstalks between the two channel waveguides can be significantly smaller. An interdigital transducer is symmetrically positioned so that the SAW generated propagates in the intersection region. The center frequency of the SAW is such that the corresponding Bragg angle is equal to one half of the intersection angle. An optical wave incident at guide 1 is diffracted by the moving optical grating induced by the SAW. Consequently, a portion of the incident light is deflected into guide 3. The frequency of the deflected light is up-shifted by an amount equal to the acoustic frequency. Similarly, an optical wave incident at guide 2 will have a portion of its intensity deflected into guide 4 and have the frequency of the deflected light down-shifted by the same amount. Such a device module should find a variety of applications in future integrated and fiber optic systems. In the application for heterodyne detection, the frequency-shifted light can be conveniently used as a reference signal (local oscillator) in connection with optical communications and fiber optic sensing.

A high diffraction efficiency was demonstrated earlier in a preliminary experiment (ref. 8) with multimode crossed-channel waveguides of 30μm channel width in a Y-Cut LiNbO$_3$ substrate and a SAW operating at 634 MHz center frequency. We have recently extended this experimental study to single-mode crossed-channel waveguides of 10μm channel width, and have obtained similarly encouraging results (ref. 6). Specifically, a 50% diffraction efficiency and a bandwidth of 13.4 MHz were obtained with 0.13 watt of acoustic power centered at 320 MHz. This result clearly indicates the feasibility for realization of an active integrated optic module with a 50-50 power split and a tunable frequency offset. Consequently, this crossed-channel AO module should find a variety of applications in integrated and fiber optic systems. Fig. 4 is a photograph of the resultant module. Located in the center of the device holder is the LiNbO$_3$ plate which has the dimensions 0.2 x 1.0 x 1.4 cm. A pair of RF connectors for excitation and detection of the SAW are also shown. While both prism-and edge-couplings of the light beam have been utilized successfully, a more rigid coupling using single-mode fibers is being pursued.

ELECTROOPTIC CROSSED CHANNEL WAVEGUIDE TIR MODULATOR AND 4 X 4 SWITCHING NETWORK

A variety of channel waveguide electrooptical (E-O) devices in LiNbO$_3$ substrates have demonstrated desirable characteristics, including low RF drive power, small sizes, and high switching speed or large modulation bandwidth. Consequently, such E-O devices should provide essential functions for realization of single-mode optical fiber communication and optical signal processing systems. One of the guided-wave E-O devices that has received increasing interest utilizes the electrically-induced total internal reflection (TIR) in a crossed-channel waveguide (ref. 9). The basic device configuration is shown in Fig. 5. The crossed-channel waveguide employed in this TIR device is similar to that employed in the channel waveguide acoustooptic device described in the last section. A pair of parallel metal electrodes are deposited in the middle of the crossover region. In absence of an applied voltage, an incident light from port 1, for example, will transmit rather freely through the layer defined by the parallel electrodes and exit at port 4. However, when a voltage of appropriate polarity is applied, the refractive index in the layer is reduced due to the linear electrooptic effect. Two refractive index interfaces are thus created electrically. A total internal reflection (TIR) of the light will occur at the first interface if the incident angle is larger than the critical angle θ_c. Therefore, if

151

the intersection angle of the channel waveguides and, consequently, the incident angle of the light beam is chosen to be in the neighborhood of the critical angle, the ratio of the reflected (switched) light power to the transmitted (unswitched) light power becomes a sensitive function of the applied voltage (ref. 9). It is clear that the very small length of the parallel electrode pair suggests a very small capacitance and thus a very large base bandwidth for the device. For example, an electrode length of 1mm and 50-ohm termination will provide a theoretical base bandwidth of 20 GHz. It was also previously shown that by using a suitable intersection angle both low drive voltage and low crosstalk could be simultaneously achieved (ref. 6).

We had earlier fabricated and tested such TIR modulators and switches in multimode crossed channel waveguides in Y-cut LiNbO$_3$ substrates (ref. 6). We have recently realized a single-mode multigigahertz bandwidth TIR modulator and a simple 4 x 4 switching network which consists of five such basic modulators, again in the Y-cut LiNbO$_3$ substrates (ref. 10). The channel width and the intersection angle of the crossed channel waveguide are 10μm and 1.5 degrees, respectively. The length of the basic modulator along the optical path is 2.2mm. The best measured results for the basic modulator at 6328 Å wavelength are a base bandwidth greater than 2.0 GHz (limited by the availability of high-speed electronics testing equipment), a drive voltage of 18 volts for 90% switching efficiency, a crosstalk of -15 dB, and an estimated insertion loss of 1 dB. A simple scheme which employs a cascade of three identical devices for reduction of the crosstalks by a factor of two in dB, namely, from -15 dB to -30 dB, was also verified experimentally.

Fig. 6 is a photograph of the finished basic modulator module and the microscope objectives at right and left for edge-coupling of the light beam in actual experiment. The LiNbO$_3$ plate and the RF connector to the coplanar microstrip transmission on it are positioned at the top and a 50-ohm termination at the bottom.

Channel waveguide optical switching networks or matrices (ref. 11,12) are expected to provide a variety of high-speed operations, such as multiport routing and multiplexing in single-mode fiber optic communication and signal processing systems. Fig. 7(A) shows the geometry of a simple 4 x 4 optical switching network which was fabricated and tested (ref. 10). The total length of the switching network along the optical path is 0.74cm. This very small dimension is attributed to the fact that all individual switches are very small along the optical path and that only straight channel waveguides are required for their interconnections.

Multiport beam switching and routing experiments were carried out with the light incident at the second input port and subsequently modulated by switch S$_1$ at 1 KHz. Routing of the light to any of the four output ports was accomplished by setting switches S$_2$, S$_4$ and S$_5$ at appropriate switching states as indicated. Since the amplitudes of all four output waveforms as shown in Fig. 7(B) are practically the same, it is reasonable to conclude that the optical insertion loss associated with each individual route is also practically the same. Furthermore, since the total lengths of channel waveguides in all routes are almost identical, it is reasonable to suggest that the insertion loss of the switch was the same for all and was estimated to be at most 1 dB. This insertion loss for the switch was determined by comparing the output waveform of the route involving switches S$_1$, S$_5$ and S$_2$. Finally, the measured crosstalks at the unintended ports are typically -15 to -17 dB.

In summary, various single-mode crossed channel waveguide TIR device configurations, including single, cascaded, and matrix modulator/switches, have been realized in a Y-cut LiNbO$_3$ substrate. A bandwidth greater than 2 GHz has been demonstrated in the single modulator. Since only straight channel waveguides are required, such

TIR devices possess the advantage of being very small in dimensions along the optical path which in turn results in very low insertion loss and high packing density. Various potential applications of such TIR devices are possible. For example, optical computation using an array of such TIR devices has been suggested (ref. 13,14). Some of the more obvious applications of such devices include high-speed multiport switching and routing in single-mode fiber optical communication and signal processing systems as well as data routing in electronic computer networks.

ELECTROOPTIC ANALOG-TO-DIGITAL CONVERTER USING CHANNEL WAVEGUIDE FABRY-PEROT MODULATOR ARRAY

One of the important signal processing applications that utilizes guided wave electrooptic (E-O) devices lies in analog-to-digital (A/D) conversion of wideband RF signals (ref. 15,16). Several types of electrooptic A/D converters which utilize guided-wave E-O devices in $LiNbO_3$ have been demonstrated (ref. 17-21).

We are currently studying a new type of E-O A/D converter (ref. 22) which utilizes an array of channel waveguide Fabry-Perot modulators (ref. 23) in a X-cut $LiNbO_3$ substrate. A 4-bit converter has been fabricated and the experimental results obtained with a He-Ne laser at 6328 Å have demonstrated some of its desirable features. The elements of this integrated E-O A/D converter are depicted in Fig. 8. A set of parallel electrode pairs to which the analog voltage is applied electrically in parallel is designed such that the electrode lengths of adjacent modulators differ by a factor of two for a binary-code representation. Activation of this apodized electrode array by the analog voltage will result in modulation of the refractive index and thus the phase shift of the light and the optical transmission characteristic in each channel waveguide. Thus an E-O Fabry-Perot modulator (ref. 24) is formed in each waveguide. It can be shown that the shape of the transmission characteristic versus the applied analog voltage or the total phase shift in each channel waveguide is periodic and its periodicity is inversely proportional to the length of the electrode. Accordingly the periodicity of modulation as a function of the applied voltage is reduced by a factor of two between adjacent channel waveguides. It is to be noted that each channel waveguide modulator is also incorporated with an electrooptic phase shifter to provide independent adjustment of its static phase shift. The depth of modulation in the transmitted light of each Fabry-Perot modulator is determined by the reflectivity of the two identical mirror facets and the attenuation coefficient in the channel waveguide. A series of plots generated by a computer calculation has shown that a significant modulation depth in the transmitted light intensity is achievable in the aforementioned $LiNbO_3$ substrate if the reflectivity of the mirrors and the optical attenuation coefficient are sufficiently low. Specifically, a reflectivity of 0.14 (which results from the difference in refractive index between the air and the X-cut $LiNbO_3$ channel waveguide) and an attenuation coefficient of up to 2.0 dB per cm are sufficient for this purpose. To summarize, the readily achievable modulation depth in the periodic dependence of the output light as a function of the applied voltage and the electrode length in a channel waveguide Fabry-Perot modulator suggests that a suitable light intensity threshold may be chosen to establish the "1" and "0" states for each element of the modulator array.

Referring to Fig. 8 again, a suitable laser diode array (ref. 25) is edge-coupled to one end face of the $LiNbO_3$ plate to provide the sampling optical pulses at a very high rate by direct modulation of injection current. At the output end an array of high-speed avalanche photodetectors, edge-coupled to the other end face of the $LiNbO_3$ plate, serve to convert the optical signals into electrical signals. If

necessary, the resultant electrical signals may also be enhanced by amplifiers. Finally, the high-speed electronic comparators which follow the amplifiers serve to compare the electrical signals with appropriate reference thresholds and generate the digital outputs.

In the experimental study, a 4-bit converter which consists of four parallel single-mode channel waveguides along the Y-axis was first designed and fabricated in a X-cut LiNbO$_3$ substrate using the conventional Ti-diffusion method (ref. 26). While the separation between adjacent waveguides is 500 µm, the separation of all electrode pairs in the apodized electrode array is 10 µm. The length of the longest electrode pair (for the LSB) is 10.0mm and the length of the static phase shifter in each waveguide is 2.0mm. Fig. 9 is a photograph of the LiNbO$_3$ substrate with the channel waveguide Fabry-Perot modulator array. A cw He-Ne laser (Fig. 10) shows the 22 KHz ramp analog test signal and the corresponding outputs from both the photomultiplier and the comparator for all bit channels of the 4-bit converter. It is seen that the period of the 2nd bit is twice that in the LSB as expected. This observation is valid for all adjacent bits. Since the maximum peak voltage of the ramp test signal was limited to 30 volts while the measured half-wave voltage for the LSB was 6.6 volts, some of the voltage levels were not digitized in this particular experiment.

In summary, a new electrooptic analog-to-digital converter which utilizes an array of channel waveguide Fabry-Perot modulators in a X-cut LiNbO$_3$ substrate has been studied using a 4-bit converter in a binary-code representation. The experimental results obtained have shown that it is feasible to fabricate Fabry-Perot modulator array with uniform quality. The length of the LiNbO$_3$ substrate used in this preliminary converter is 2.5cm; however, it can be easily reduced to 1.5cm in future design. Although this preliminary converter would require a peak-to-peak voltage of 52.8 volts to generate all digital words, this voltage requirement can be easily reduced by a factor of four in future design. Since only straight channel waveguides are required, this type of E-O A/D converter should possess the inherent advantages of simple geometrical layout, small substrate size, and low optical insertion loss as the number of bit precision is higher than, say, four. A preliminary analysis indicates that such converters should be capable of providing 1 GHz sampling rate with six to eight bits precisions.

NONCOLLINEAR MAGNETOOPTIC MODULATOR USING MAGNETOSTATIC SURFACE WAVE

Magnetostatic Surface Waves (MSSW) result from the electron spins precessing around a DC magnetic field but with its energy confined in a thin layer of ferromagnetic material such as YIG (Yttrium iron garnet) on a suitable substrate such as GGG (Gadolinium gallium garnet). MSSW can be readily generated by applying a microwave signal to a short-circuited metallic strip. The center frequency of the MSSW can be simply tuned, typically from 1.0 to 20 GHz, by varying an external DC magnetic field (ref. 27-29). Other potential advantages of the MSSW in comparison to the SAW include: 1) simple transducers not requiring critical photolithography, typically 50 µm wide; 2) lower propagation losses at the higher frequencies; and 3) both dispersive and nondispersive properties of the magnetostatic waves can be utilized. Since, like the SAW, the MSSW will induce a moving optical grating in the YIG film waveguide, a guided-light wave can be modulated by diffraction.

An interaction configuration of particular interest that has been identified is shown in Fig. 11. Note that in this non-collinear configuration, the propagation

direction of the lightwave is nearly orthogonal to that of the MSSW, in contrast to the collinear configuration (in which the light waves and the MSSE propagate in the same line) that was recently reported (ref. 30). Like guided-wave acoustooptics, non-collinear guided-wave magnetooptic interactions are expected to be much more versatile in application than the collinear interactions.

The dimensions of the YIB/GGG waveguide and the MSSW are shown in Fig. 11. A DC magnetic field of about 600 Gauss was applied to excite a MSSW with the center frequency at 3.9 GHz. Fig. 12 shows the waveform of the square-wave modulated light at 1.15 μm wavelength. An RF bandwidth of 250 MHz and a dynamic range of 15 dB have been measured in this preliminary experiment. Refined experiments are in progress.

In summary, noncollinear guided-wave magnetooptic diffraction using magnetostatice surface waves has been observed for the first time. This diffraction phenomenon should result in a number of integrated optic devices for wideband communication and signal processing systems with a center frequency much higher than that of acoustooptic devices.

CONCLUSION

Encouraging performance figures in terms of base bandwidth and device substrate sizes have been experimentally demonstrated with four single-mode hybrid integrated optic device modules in $LiNbO_3$ waveguide substrates and one in YIG/GGG substrates. Consequently, such device modules should act as efficient interface devices between a light wave and wideband temporal signals in optical communication and real-time signal processing systems. Although the present fabrication yield of such $LiNbO_3$-based modules has been less than desirable, increased yield should be possible through improvement in fabrication skills and facility. Both prism- and edge-couplings have been successfully employed to couple the He-Ne laser light at 6328 Å and 11500 Å wavelengths to the waveguide substrates. However, such coupling methods required delicate and time-consuming alignment and adjustment. A more robust approach, such as fiber-waveguide coupling, should enhance the practicality and utility of such device modules. Finally, a total hybrid integration of the devices requires coupling of a single-diode laser or an array of the same to the waveguide substrate. Such diode lasers should also greatly reduce the susceptibility of the devices to optical damage.

REFERENCES

1. I.W. Yao and C.S. Tsai, "A Time-Integrating Correlator Using Guided-Wave Acousto-optic Interactions," _1978 IEEE Ultrasonics Symposium Proc._, pp. 87-90, IEEE Cat. No. 78CH1344-1SU.

2. C.S. Tsai, J.K. Wang and K.Y. Liao, "Acoustooptic Time-Integrating Correlators Using Integrated Optics Technology." _SPIE-Symp. on Real-Time Signal Processing II_, _SPIE_, Vol. 180, pp. 160-162, 1979.

3. K.Y. Liao, C.C. Lee and C.S. Tsai, "Time-Integrating Correlator Using Guided-Wave Anisotropic Acoustooptic Bragg Diffraction and Hybrid Integration," _1982 Topical Meeting on Integrated and Guided-Wave Optics_, Jan. 6-8, 1982, Pacific Grove, CA., _Technical Digest_, pp. WA4-1 to -4, IEEE Cat. No. 82CH1719-4.

4. C.C. Lee, K.Y. Liao, and C.S. Tsai, "Acoustooptic Time-Integrating Correlator Using Hybrid Integrated Optics," _1982 IEEE Ultrasonics Symp. Proc._, pp. 405-407, IEEE Cat. No. 82CH1823-4.

5. C.S. Tsai, "Guided-wave acoustooptic Bragg modulators for wide band integrated optic communications and signal processing," _IEEE Trans. Circuits and Systems_, Vol. _CAS-26_, 1072-1098 (Dec. 1979).

6. C.S. Tsai, C.T. Lee, and C.C. Lee, "Efficient Acoutooptic Diffraction in Crossed Channel Waveguides and Resultant Integrated Optic Module," _1982 IEEE Ultrasonics Sym. Proc._, IEEE Cat. No. 82CH1823-4, pp. 422-425.

7. F.R. El-Akkari, C.L. Chang and C.S. Tsai, "Electrooptical Channel Waveguide Matrix Switch Using Total Internal Reflection," _Topical Meeting On Integrated and Guided Wave Optics_, Jan. 28-30, 1980, Incline Village, Nevada. _Technical Digest_, pp. TuE 4-1 to -4, IEEE Cat. No. 80CH1489-4QEA.

8. C.S. Tsai, C.L. Chang, C.C. Lee, and K.Y. Liao, "Acoustooptic Bragg Deflection in Channel Optical Waveguides," _1980 Topical Meeting on Integrated and Guided-Wave Optics, Technical Digest of Post Deadline Papers_, pp. PD7-1 to -4, IEEE Cat. No. 80CH1489-4QEA.

9. C.S. Tsai, B. Kim, and F.R. El-Akkari, "Optic Channel Waveguide Switch and Coupler Using Total Internal Reflection," _IEEE J. Quantum Electron._, Vol. _QE-14_, 513-517 (1978).

10. C.L. Chang and C.S. Tsai, "GHz Bandwidth Optical Channel Waveguide TIR Switches And 4x4 Switching Networks," _1982 Topical Meeting on Integrated and Guided-Wave Optics_, Jan. 6-8, Pacific Grove, CA, _Technical Digest_, pp. ThD-1 to -4, IEEE Cat. No. 82CH1719-4.

11. H.F. Taylor, "Optical Waveguide Connecting Networks," _Electron. Lett._, Vol. QE-14, 513-517 (1978).

12. R.V. Schmidt, "Experimental 4x4 Optical Switching Network." _Electron. Lett._, Vol. _12_, 575-577 (1976).

13. A. Huang, Y. Tsunoda, J.W. Goodman, and S. Ishihara, "Optical Computers Using Residue Arithmatics," _Appl. Opt._, Vol. 18, pp. 149-159 (1979).

14. J.N. Polky and D.D. Miller, "Optical Waveguide Circuit Design of an Adaptive Filter in the Residue Number System," Appl. Opt., Vol. 21, pp. 3539-3551 (1982).

15. S. Wright, I.M. Mason, and M.G. Wilson, "High-Speed Electrooptic Analogue-Digital Conversion," Electron. Lett., Vol. 10, pp. 508-509, Nov. 28, 1974.

16. H.F. Taylor, "An Electrooptic Analog-To-Digital Converter," Proc. IEEE, Vol. 63, pp. 1524-1525, Oct. 1975.

17. P. Saunier, C.S. Tsai, I.W. Yao, and Le T. Ngugen, "Electrooptic Phased-Array Light Beam Deflector With Application To Analog-To-Digital Converter," 1978 Topical Meeting on Integrated and Guided-Wave Optics, Jan. 16-18, Salt Lake City, Utah, Technical Digest, pp. TuC 2-1 to 2-4, IEEE Cat. No. 78CH1280-7.

18. H.F. Taylor, M.J. Taylor, and D.W. Bauer, "Electro-Optic Analog-To-Digital Conversion Using Channel Waveguide Modulators," Appl. Phys. Lett., Vol. 32, pp. 559-561, 1978.

19. C.D.H. King and J.D. Jackson, Proc. 6th European Conf. on Opt. Comm., 256, 1980.

20. F.J. Leonberger, C.E. Woodward, and R.A. Becker, "4-bit 828 Megasample/s Electro-Optic Guided Wave Analog-To-Digital Converter," Appl. Phys. Lett., Vol. 40, pp. 565-568, 1982.

21. S. Yamada, M. Minabata, and J. Noda, "High Speed 2-Bit Analogue-Digital Converter Using LiNbO$_3$ Waveguide Modulator," Electron Lett., Vol. 17, pp. 259-260, 1981.

22. C.L. Chang and C.S. Tsai, "An Integrated Optical Analog-To-Digital Converter Using An Array of Channel Waveguide Fabry-Perot Modulators," Paper presented at the International Conference on Integrated Optics and Optical Fiber Communication, June 27-30, 1983, Tokyo, Japan.

23. P.W. Smith, I.P. Kaminow, P.J. Maloney, and L.W. Stulz, "Integrated Bistable Optical Devices," Appl. Phys. Lett., Vol. 33, pp. 24-26, 1978.

24. E.I. Gordon and J.D. Rigden, "The Fabry-Perot Electrooptic Modulator," Bell Syst. Tech. Jour., Vol. 42, pp. 155-179, 1963.

25. D. Botex, J.C. Connolly, D.B. Gilbert , M.G. Harvey, and M. Ettenberg, "High-Power Individually Addressable Monolithic Array of Constricted Double Heterojunction Large-Optical-Cavity Lasers," Appl. Phys. Lett., Vol. 41, pp. 1040-1042, 1982.

26. R.V. Schmidt and I.P. Kaminow, "Metal Diffused Optical Waveguides In LiNbO$_3$," Appl. Phys. Lett., Vol. 25, pp. 458-460, 1974.

27. J.D. Adam and J.H. Collins, "Microwave Magnetostatic Delay Devices Based on Epitaxial Yttrium Iron Garnet," Proc. IEEE, 64, 794-800 (May 1976).

28. J.M. Owens, R.L. Carter, C.V. Smith and J.H. Collins, "Magnetostatic Waves, Microwave SAW," 1980 IEEE Ultrasonics Symp. Proc., Cat. No. 80C1602-2, 506-513.

29. L.R. Adkins and H.L. Glass, "Propagation of Magnetostatic Surface Waves in Multiple Magnetic Layer Structures, "Electronics Letters, Vol. 16, No. 15, 590-592 (July 17, 1980).

30. A.D. Fisher, J.N. Lee, E.S. Gaynor, and A.B. Tveten, "Optical Guided-Wave Interactions with Magnetostatic Waves at Microwave Frequencies," _Appl. Phys. Lett._, Vol. 41, pp. 779-781 (Nov. 1982).
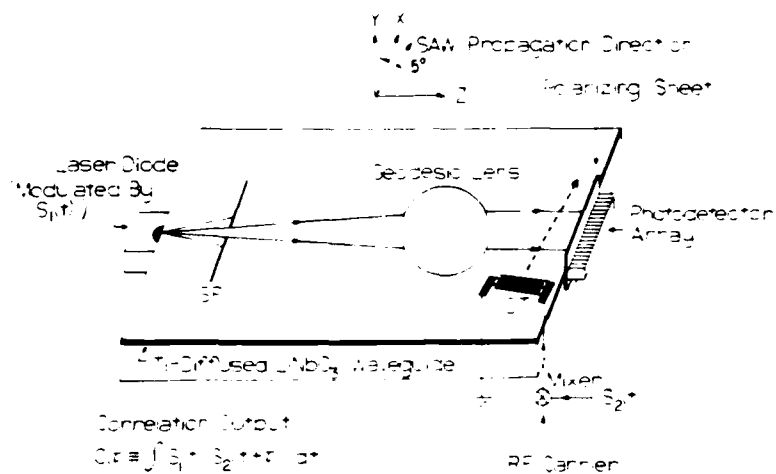
Figure 1.- Acoustooptic time-integrating correlator using anisotropic
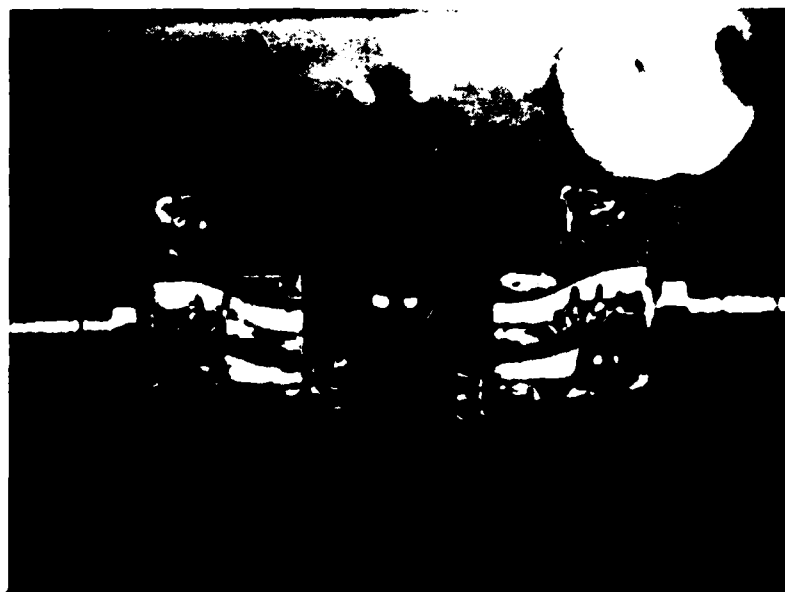Bragg diffraction and hybrid optical waveguide structure.

Figure 2.- Hybrid integrated module for acoustooptic time-integrating
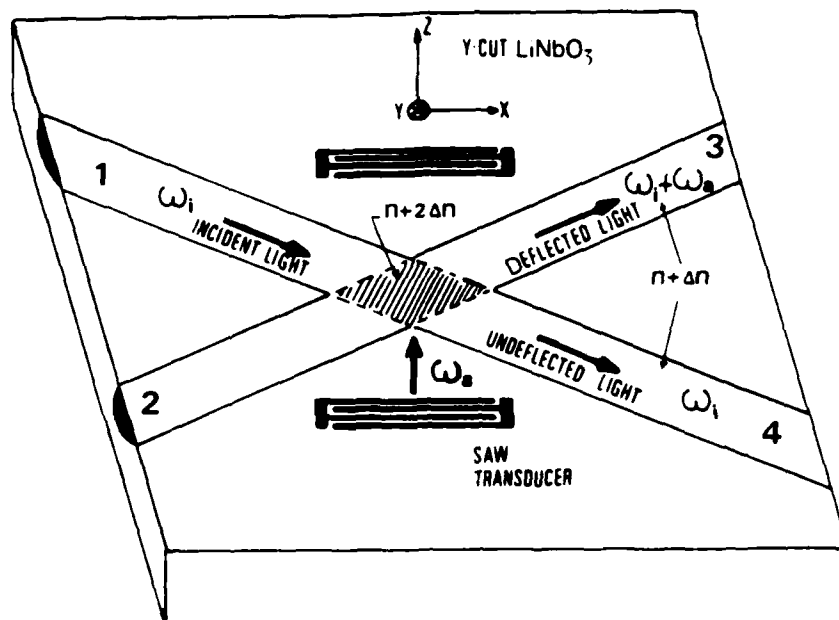correlation.

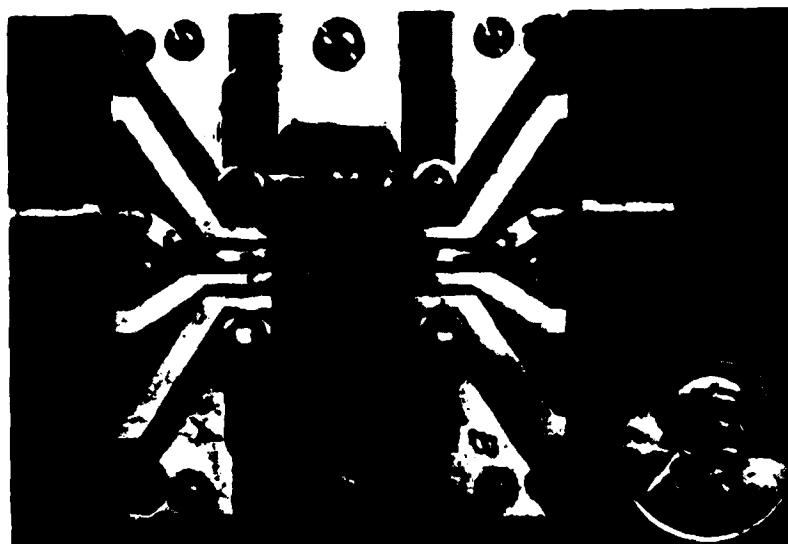Figure 3.- Acoustooptic diffraction from surface acoustic wave in
crossed-channel waveguides.

Figure 4.- Single-mode crossed-channel waveguide acoustooptic modulator/
deflector in LiNbO$_3$ substrate.
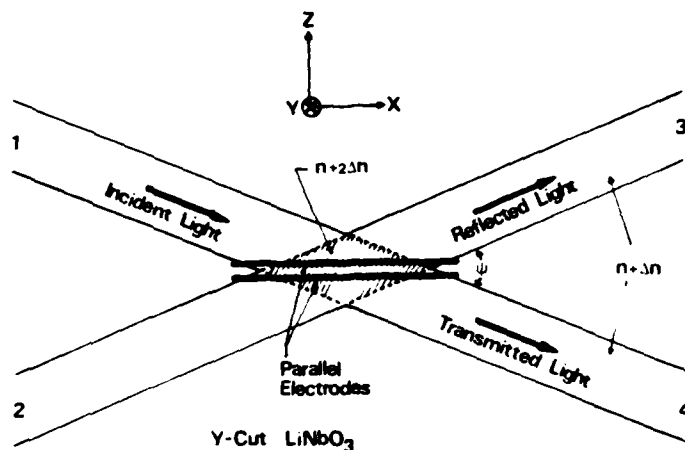
Figure 5.- Electrooptic total internal reflection in crossed-channel
waveguide in LiNbO$_3$ substrate.
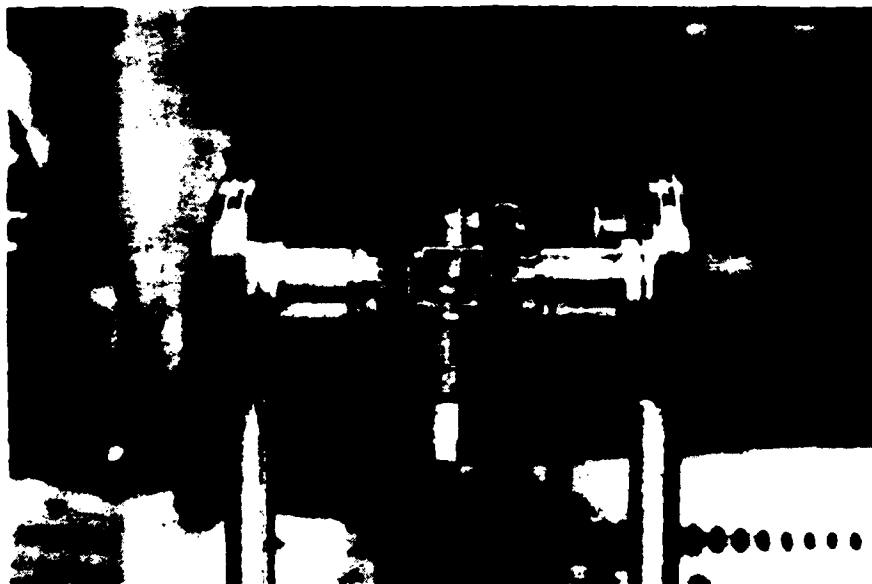
Figure 6.- Basic electrooptic TIR modulator/switch module in crossed-
channel waveguide showing LiNbO$_3$ plate in Middle and Microscope
objectives at right and left for edge-coupling of light beam.
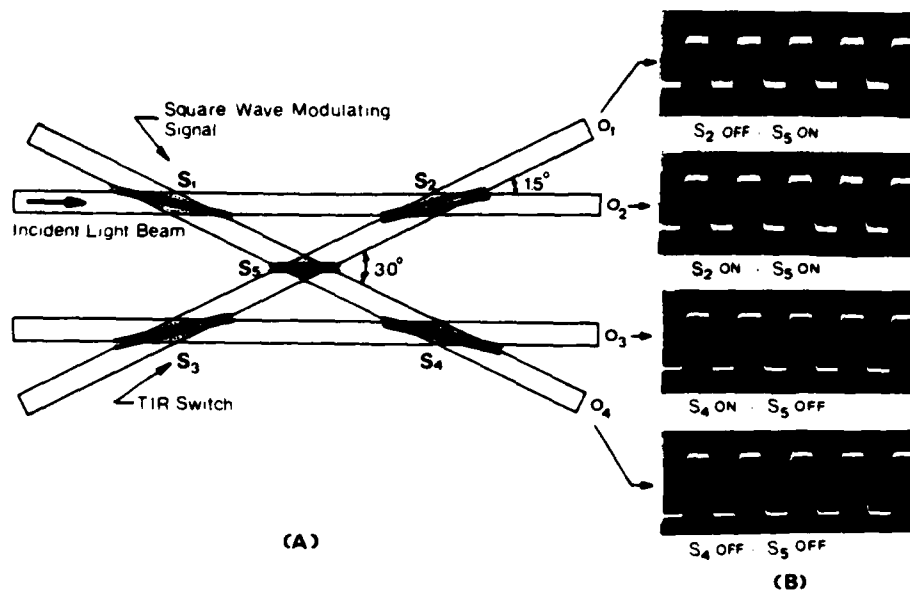
Figure 7.- 4 x 4 optical switching network using crossed-channel waveguide
TIR switches (A) and output waveforms for four switching states (B).
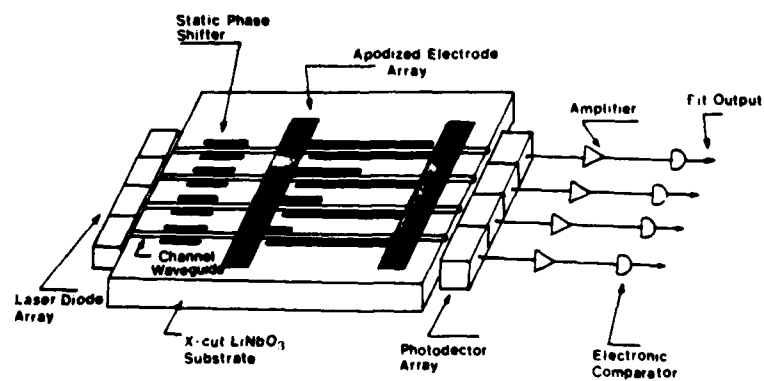
Figure 8.- Schematic diagram of electrooptic A/D converter utilizing array
of Fabry-Perot modulators.
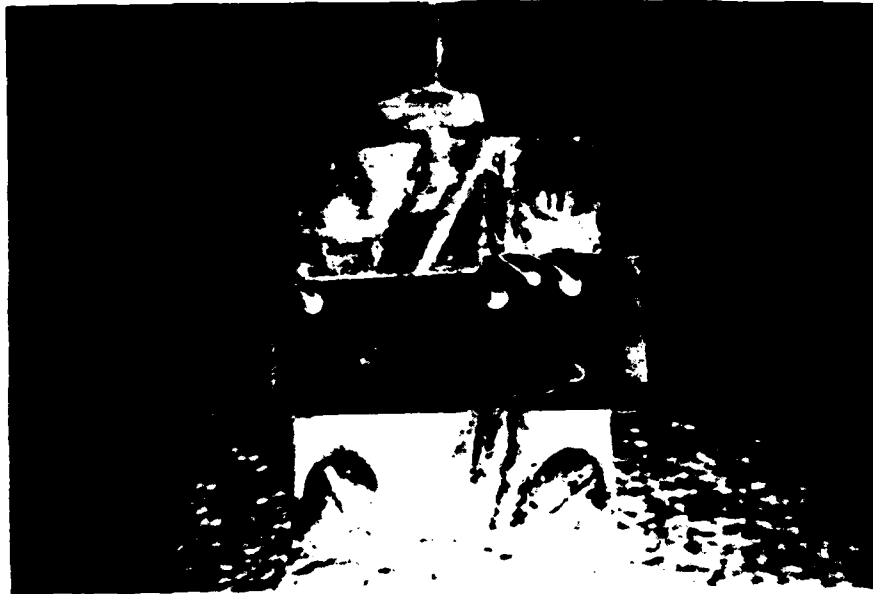
Figure 9.- Photograph showing LiNbO$_3$ plate with four parallel channel
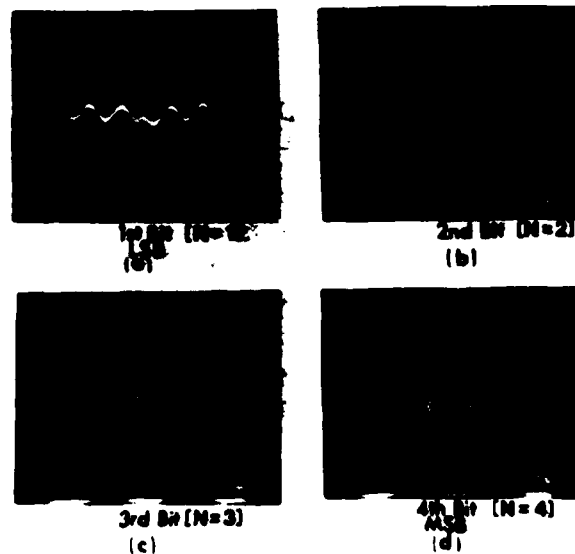waveguide Fabry-Perot modulators for analog-to-digital conversion.

Figure 10.- Experimental results of a 4-bit electrooptic A/D converter
using channel waveguide Fabry-Perot modulator array in figs
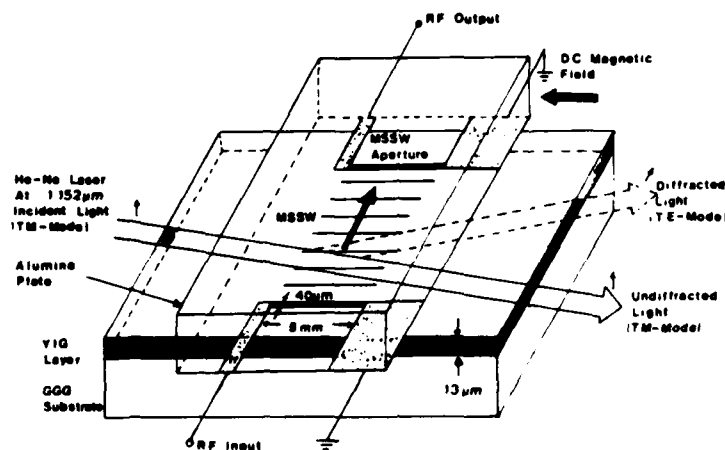(a) to (d).

Figure 11.- Device geometry for guided-wave noncollinear anisotropic magneto-optical diffraction using magnetostatic surface wave.
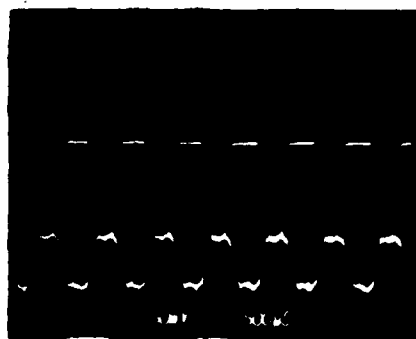

Figure 12.- Guided-wave noncollinear anisotropic magnetooptic diffraction from magnetostatic surface wave: 1.4 KC square-wave modulated magnetostatic surface wave at 3.9 GHz carrier frequency (top trace); diffracted light waveform (bottom trace).

Chen Tsai

FOURTH INTERNATIONAL CONFERENCE

ON

INTEGRATED OPTICS

AND

OPTICAL FIBER COMMUNICATION

Main Conference

Technical Digest

IOOC '83
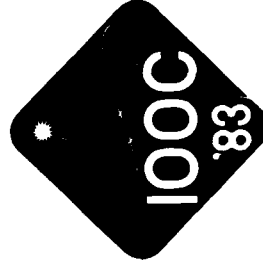
June 27 - 30, 1983

Tokyo, Japan

EFFICIENT WIDEBAND ACOUSTOOPTIC BRAGG DIFFRACTION IN GaAs-GaAlAs WAVEGUIDE STRUCTURE*

C.J. Lii, C.C. Lee, O. Yamazaki(1), L.S. Yap,
K. Wasa(1), J. Merz(2), and C.S. Tsai

School of Engineering
University of California
Irvine, CA 92717, U.S.A.

In comparison to the LiNbO₃ substrate the GaAs substrate provides a greater future potential for integration of active and passive components that are required in information processing and communications applications. One of the key components in such future GaAs integrated optic circuits is an efficient wideband acoustooptic (AO) modulator or deflector[1].

Unlike LiNbO₃ the piezoelectricity of GaAs is rather weak, however. Sputtered ZnO overlay films are thus required for efficient excitation of surface acoustic waves (SAW)[2]. In fact, such piezoelectric film was used in an earlier study on guided-wave AO interactions in GaAs[3]. Most recently, some results of a preliminary study on guided-wave AO interactions in a Z-cut GaAs/GaAlAs waveguide structure as shown in Fig. 1 were reported by us[4]. It was shown theoretically that <100>- and <110>-propagating SAWs are capable of providing very large Ao Bragg bandwidth, namely, 1.6 GHz, respectively, for a 0.4 μm waveguide supporting TE₀ mode at 1.15 μm optical wavelength. A preliminary experiment carried out with edge-coupling of the light beam at 1.15 μm and a 1.0 mm-aperture SAW at 200 MHz also demonstrated a high diffraction efficiency, namely, 50% diffraction at 47 mw rf drive power. We have since continued theoretical and experimental studies on the subject and have obtained additional results. In this paper some of these most recent results are reported.

On the theoretical side we have completed a detailed coupled-mode analysis[5,6] and formulated a computer program to evaluate the diffraction efficiency and the Ao Bragg bandwidth for various combinations of crystal orientations and SAW propagation directions

including those referred to above. For example, as shown in Fig. 2(a) and 2(b) the topographical distribution of the induced change in dielectric constant created by the <121>-propagating SAW in the (111)-substrate differs drastically from that created by the <100>-propagating Saw in the (001)- substrate. The nodal planes are seen to be flat in Fig. 2(a) but not in Fig. 2(b). The effects of this observation are reflected in the corresponding frequency dependence of the acoustic power-beam width product (PI) as shown in Fig. 3(a) and 3(b), exhibiting a phase cancellation in the former but not in the latter. However, from Figs. 4(a) and 4(b) the inherent AO Bragg bandwidth in the two interaction configurations are rather similar. In summary, a comparison of the various combinations of crystal orientations and SAW propagation directions in terms of the optical waveguide mode, the diffraction efficiency, the AO Bragg bandwidth, the beam steering, and the possible conversion of the SAW mode to the leaky mode will be presented.

On the experimental side both the RF-magnetron sputtering system[7] and the LPE system are being improved to produce, respectively, ZnO films and GaAs/GaAlAs waveguides of higher quality. Realization of efficient wideband Bragg modulators and deflectors using multiple-tilted transducers[1] for excitation of <100>-propagating SAW in the (001)-substrate is in progress. As in the preliminary experiment referred to earlier the (110) cleaved plane is being used to edge-couple both input and output single-mode beams at 1.15 μm. The results of this experimental sutdy will also be reported.

ACKNOWLEDGEMENTS

REFERENCES

[1] See for Example, C.S. Tsai, IEEE Trans. Circuits and Systems, Vol. CAS-26, No. 12, pp. 1072-1098, Dec., 1979.

[2] T.W. Grudkowski, G.K. Montress, M. Gilden and J.F. Black, 1980 Ultrasonics Symposium Proceedings, pp. 88-97, 1980.

[3] K.W. Loh, W.S. C. Chang, N.R. Smith, and T. Grudkowski, Appl. Opt., Voo. 15, No. 1, pp. 156-166, January, 1976.

[4] O. Yamazaki, C.C. Tsai, M. Umeda, L.S. Yap, C. J. Lii, K. Wasa, and J. Merz, Presented at the 1982 IEEE Ultrasonics Symposium, Oct. 27-29, San Diego, CA.

[5] A. Yariv, "Introduction to Optical Electronics", 2nd Edition, Holt, Rinehart and Winston New York, 1976.

[6] Y. Ohmachi, J. Appl. Phys. Vol. 44, pp. 3928-3933, 1973.

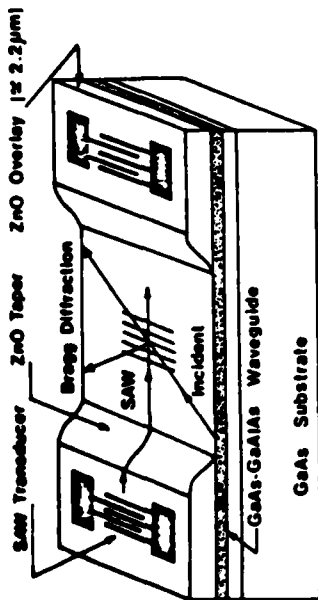[7] O. Yamazaki, K. Wasa and S. Hayakawa, 1980 Ultrasonics Symposium Proceedings, pp. 382-385, 1980.

Fig.3 SAW Power Density Required for 100% Diffraction V.S. Waveguide Thickness In Micron

400 MHz
200 MHz
100 MHz
800MHz

Optical Wavelength: 1.15 μm
⟨12⟩-propagating SAW On
(111)-Substrate

Acoustic Power — Beam Width Product PL (Wm)

Optical wavelength: 1.15μm
⟨100⟩-Propagating SAW On
(001)-Substrate
800MHz
400 MHz
200MHz

(b) Waveguide Thickness in Micron

Fig. 4 SAW Power Density Required V.S. Acoustic Frequency For TE₀—TE₀, 100% Bragg Diffraction In A Single—Mode Waveguide

ACOUSTIC FREQUENCY (MHz)

Acoustic Power—Beam Width Product PL (Wm)

Optical Wavelength: 1.15μm
⟨121⟩ - Propagating SAW On
(111)-Substrate
(b)

0.7μm
0.6μm
0.3μm
0.5μm
0.4μm

Optical Wavelength: 1.15μm
⟨100⟩-Propagating SAW On
(001)-Substrate
(a)

0.7μm
0.6μm
0.3μm
lₒ = 0.4μm
0.5μm

Fig.1   Guided-Wave Acoustooptic Bragg Diffraction In
        GaAs/GaAlAs-ZnO Composite Structure

Bragg Transducer   ZnO Taper   ZnO Overlay (≈ 2.2μm)

Bragg Diffraction
SAW
Incident
GaAs-GaAlAs Waveguide
GaAs Substrate

THE ⟨121⟩—DIRECTION OF PROPAGATION
IN WAVELENGTH FOR (111)—SUBSTRATE

THE ⟨100⟩—DIRECTION OF PROPAGATION
IN WAVELENGTH FOR (001)—SUBSTRATE
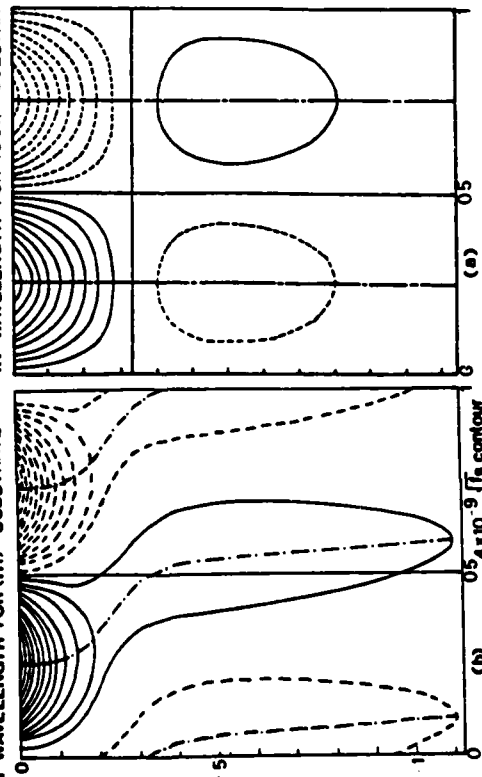(a)

(b)
—— 4x10⁻⁹ √Pₛ contour
---- 4x10⁻⁹ √Pₛ contour

Fig. 2 Topographical Distribution For The Change Of Dielectric Constant In GaAs Waveguide. The Vertical Axis In Both Figures Designates Waveguide Depth
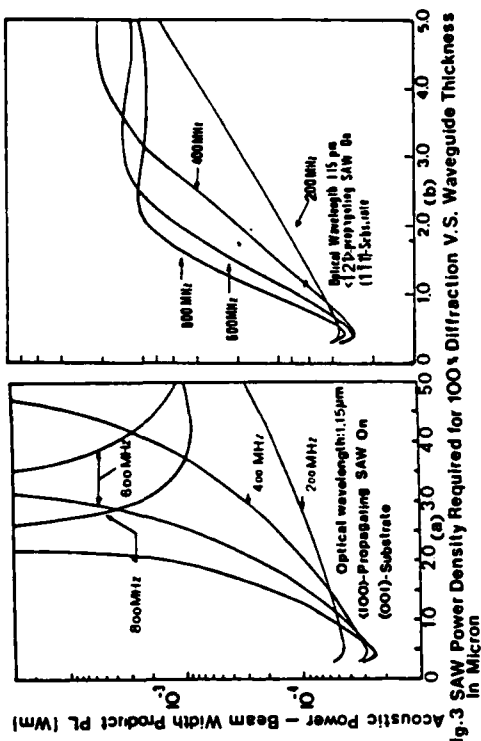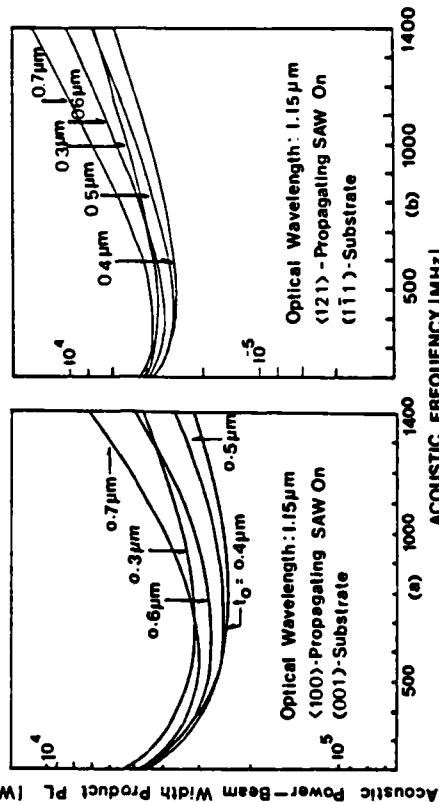
shown in Fig. 11. Note that in this non-collinear configuration, the

END
DATE
FILMED

10-8

DTIC